

AEROMAGNETIC STUDY OF THE COLORADO  
RIVER DELTA AREA, MEXICO

by

Mauricio Fernando Francisco De la Fuente Duch

---

A Thesis Submitted to the Faculty of the  
DEPARTMENT OF GEOSCIENCES

In Partial Fulfillment of the Requirements  
For the Degree of

MASTER OF SCIENCE

In the Graduate College

THE UNIVERSITY OF ARIZONA

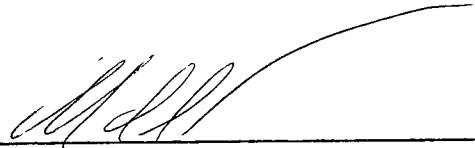
1 9 7 3

STATEMENT BY AUTHOR

This thesis has been submitted in partial fulfillment of requirements for an advanced degree at The University of Arizona and is deposited in the University Library to be made available to borrowers under rules of the Library.

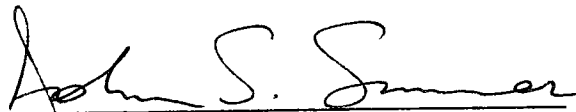
Brief quotations from this thesis are allowable without special permission, provided that accurate acknowledgment of source is made. Requests for permission for extended quotation from or reproduction of this manuscript in whole or in part may be granted by the head of the major department or the Dean of the Graduate College when in his judgment the proposed use of the material is in the interests of scholarship. In all other instances, however, permission must be obtained from the author.

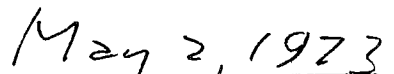
SIGNED: \_\_\_\_\_



APPROVAL BY THESIS DIRECTOR

This thesis has been approved on the date shown below:

  
\_\_\_\_\_  
JOHN S. SUMNER  
Professor of Geosciences  
and Geophysics

  
\_\_\_\_\_  
Date

## ACKNOWLEDGMENTS

I am most grateful to Dr. John S. Sumner for his sound advise. He proposed the problem to me, was the navigator-pilot, and covered all the expenses of the flights. His assistance and guidance provided the necessary stimulation for the development of this work.

For his help and the use of his computer programs, I want to thank Dr. Kenneth L. Zonge. Drs. John R. Sturgul and Spencer R. Titley provided useful comments and suggestions.

This thesis was supported by the Consejo de Recursos Naturales No Renovables (CRNNR) and by the Consejo Nacional de Ciencia y Tecnologia (CONACYT). A special mention must be made of Ing. Guillermo P. Salas, Director of the CRNNR, and Ing. Juan Jose Martinez B., Chief of the Department of Geophysics of the CRNNR, for their generous help.

My fellow students, Carlos L. V. Aiken, James B. Fink, and Ronald Peterson, helped by their discussions of several topics.

Without the encouragement and understanding of my wife, Marcia, and the vivacious presence of my daughter, Laura, this work could never have been completed.

## TABLE OF CONTENTS

	Page
LIST OF ILLUSTRATIONS . . . . .	v
LIST OF TABLES . . . . .	vii
ABSTRACT . . . . .	viii
INTRODUCTION . . . . .	1
Purpose . . . . .	1
Previous Geophysical Work in the Area and Its Vicinity . . . . .	2
GEOLOGY . . . . .	7
THEORETICAL BASIS OF THE AEROMAGNETIC METHOD . . . . .	15
Rock Magnetism . . . . .	15
Geomagnetic Field . . . . .	18
AEROMAGNETIC SURVEY . . . . .	20
Data Collection . . . . .	20
Data Processing . . . . .	21
INTERPRETATION . . . . .	27
Brief Description of the Aeromagnetic Map . . . . .	27
Magnetizations . . . . .	28
Trend Analysis . . . . .	30
Modeling . . . . .	32
Crosscorrelation . . . . .	36
Conclusions . . . . .	40
RECOMMENDATIONS . . . . .	44
SELECTED BIBLIOGRAPHY . . . . .	46

## LIST OF ILLUSTRATIONS

Figure		Page
1.	Bouguer Gravity Map of the Colorado River Delta Area . . . . .	3
2.	Aeromagnetic Map of the Salton Sea Geothermal Area . . . . .	4
3.	Total Field, Residual Aeromagnetic Map of the Head of the Gulf of California . . . . .	5
4.	Location of the Colorado River Delta Area, Mexico . . .	8
5.	Reconnaissance Geologic Map of the Mexicali Trough . . . . .	10
6.	Generalized Stratigraphic Column of the Colorado River Delta Area. . . . .	11
7.	Map of the Colorado River Delta Area Showing Location of the Major Strike-slip Faults . . . . .	13
8.	Idealized System of Spreading Centers and Compensating Right-lateral Strike-slip Faults in the Colorado River Delta Area. . . . .	14
9.	International Geomagnetic Reference Field Which Was Removed from the Original Total Magnetic Intensity Data . . . . .	23
10.	Sample of Computer-generated Plot of Flight Lines with Manual Contouring . . . . .	24
11.	Flow Chart of Procedure Followed in Constructing the Residual Total Intensity Aeromagnetic Map of the Colorado River Delta Area. . . . .	25
12.	Residual Aeromagnetic Map of the Colorado River Delta Area, Mexico. . . . . in pocket	
13.	Rose Diagram Illustrating the Results of a Trend Direction Compilation from the Aeromagnetic Map . . . . .	31

LIST OF ILLUSTRATIONS--Continued

Figure		Page
14.	Residual Aeromagnetic Map of the Colorado River Delta Area, Mexico, Showing the Location of the Magnetic Intensity Profiles . . . . .	33
15.	Total Field Profile and Model Geologic Section for Profile A-A' . . . . .	35
16.	Total Field Magnetic Profiles Used for Cross-correlation Analysis . . . . .	38
17.	Relation between Geologically Inferred Faults and Crosscorrelated Locations . . . . .	39
18.	Epicenter Locations in the Northern Baja California Area for Earthquakes Occurring during April and May 1969 . . . . .	42
19.	Location of the Panga de Abajo Spreading Center, Baja California, Mexico . . . . .	43

LIST OF TABLES

Table	Page
1. Magnetic Susceptibilities of Some Common Rock Types . .	17
2. Induced and Remanent Magnetizations for Different Major Rock Units . . . . .	29

## ABSTRACT

An aeromagnetic study of the Colorado River delta area, Baja California, Mexico, was undertaken to determine the basement structure under relatively nonmagnetic sediments and to compare magnetic values with the rock type in outcrop areas. From an economic point of view, there is a close relationship between basement structure and lithology and geothermal heat sources. From an academic point of view this study can also relate the basement structure with spreading centers.

The Colorado River delta area was flown in July 1971, using a flight-line spacing of 5 km and a constant barometric elevation of 2,000 feet (0.610 km) above mean sea level over most of the area. The barometric elevation over the mountains was 2,500 feet (0.762 km). The residual aeromagnetic map of the area was obtained by subtracting the International Geomagnetic Reference Field from the total intensity magnetic values.

The major result of this work is the discovery of an apparent spreading center, herein named Panga de Abajo, at lat  $32^{\circ}2'$  N., long  $115^{\circ}12'$  W. The association of this probable spreading center with a geothermal field could not be established with this survey. However, the aeromagnetic survey places bounds on a new area that should be studied in the future, using more detailed geophysical methods.



## INTRODUCTION

One of the most important energy sources for the ever-increasing necessity of the world is geothermal. Perhaps the most important geothermal field in Mexico is the Cerro Prieto geothermal field. Considered by Facca (1966) as the largest known geothermal field in the world in terms of areal extent and estimated reservoir volume, this field is not alone in the Colorado River delta area. Several areas showing geothermal activity have been located on the United States side of the delta.

To be optimally economic a geothermal field requires a favorable subsurface environment. This environment is formed by: (1) a heat source, (2) a reservoir, and (3) a cap rock. The cap rock and the reservoir of the geothermal fields located in the Colorado River delta area are formed by sedimentary layers of varying characteristics; the origin and nature of the heat source are still under investigation. However, it is not the purpose of this study to analyze the different concepts proposed.

### Purpose

The presence of geothermal fields in the Colorado River delta area and the importance of locating new ones provide a basis for study of the basement-sediment contact and the structure of the area. This study is the main objective of this investigation. Perhaps the most appropriate and economical preliminary method for this exploration is an aeromagnetic study. A second goal of this research was the study of the tectonic activity of the area, which is considered by several authors as one of the most tectonically active areas in the world.

Previous Geophysical Work in the Area  
and Its Vicinity

The Colorado River delta area has been studied in the past, using almost every geophysical method. This is especially true for the United States side of the delta.

On the Mexican side of the delta, the most important geophysical work was conducted by the Comision Federal de Electricidad (C.F.E.). This work was related primarily to the study of the Cerro Prieto geothermal field. Some results have been published and others remain in the C.F.E. files. Studies include gravity (Velasco H., and Martinez B., 1970), aeromagnetism (Evans, 1972), refraction seismology, and heat-flow measurements.

A regional gravity survey on the Mexican side of the delta was reported by Kovach and Monges (1961). Because of the inadequate base map available, the precision is estimated to be 1 mgal, although some measurements may be in error by more than 1 mgal. The possible error in elevation is estimated to be 15 feet, and the horizontal error ranges from 500 to 1,000 feet (Fig. 1).

As previously mentioned, the United States side of the delta has been studied in more detail. The most complete study was reported by Kovach, Allen, and Press (1962). A more recent work is the aeromagnetic study of the Salton Sea area by Griscom and Muffler (1971). Many other studies have been made in the geothermal areas in this part of the delta.

The east side of the area has been studied by J. R. Sumner (1971). His report includes gravity and aeromagnetic studies used to

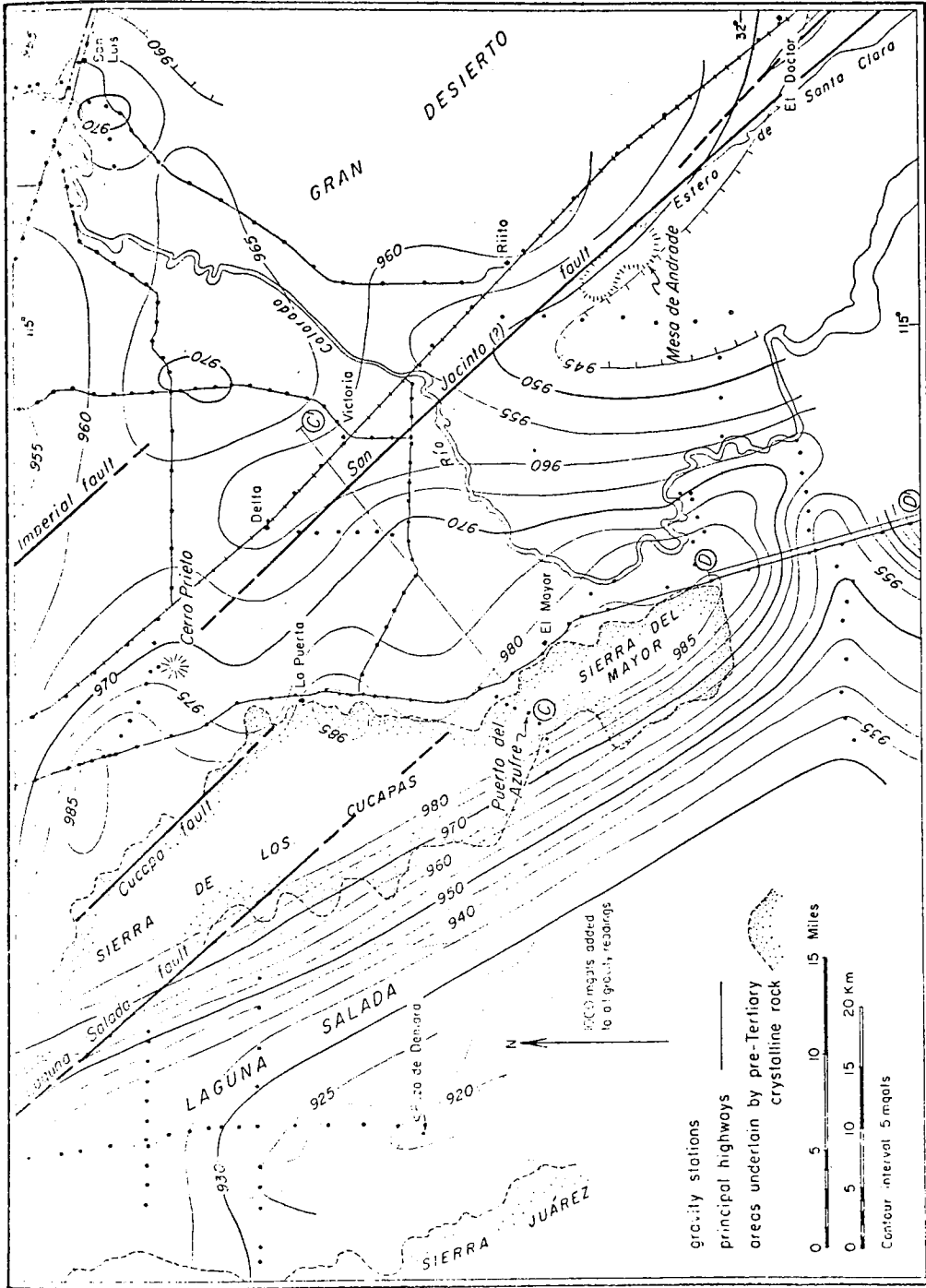


Figure 1. Bouguer Gravity Map of the Colorado River Delta Area. ---From Kovach and others (1962)

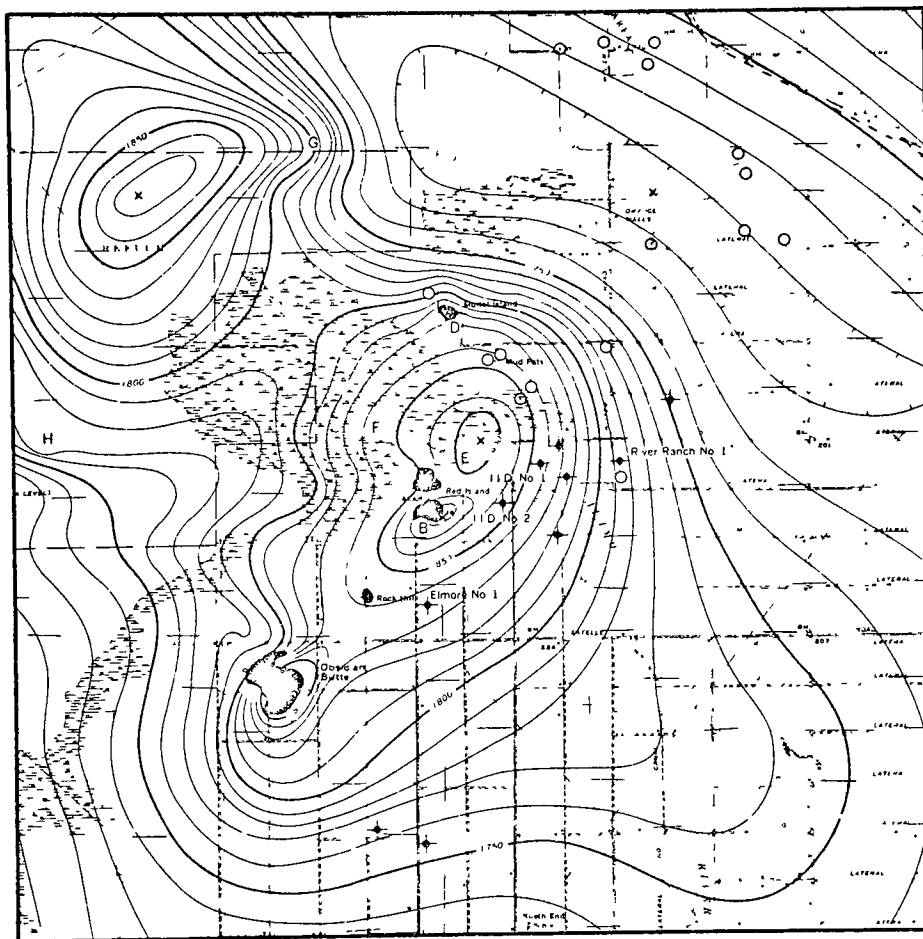


Figure 2. Aeromagnetic Map of the Salton Sea Geothermal Area.--After Griscom and Muffler (1971)

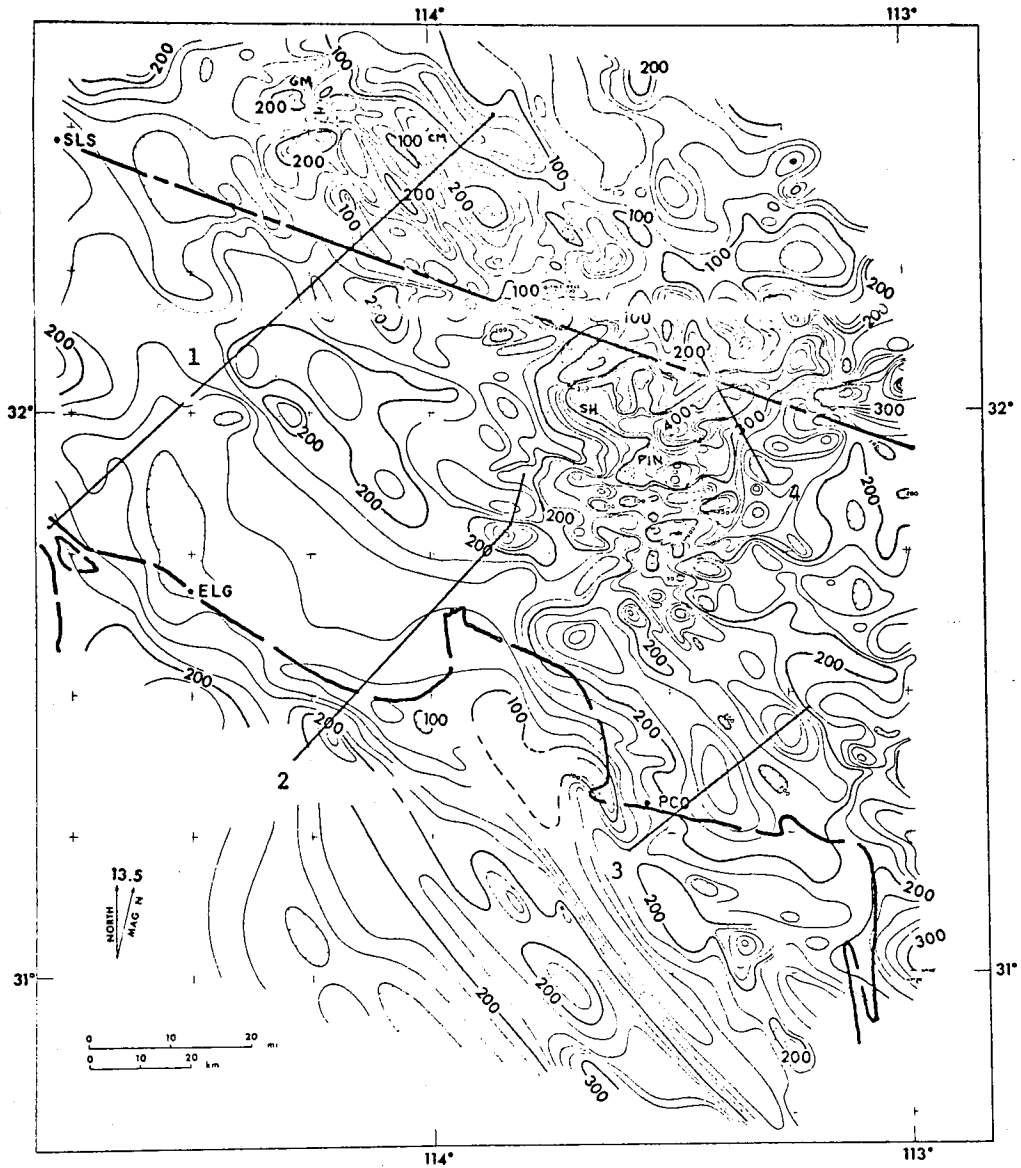


Figure 3. Total Field, Residual Aeromagnetic Map of the Head of the Gulf of California.--From J. R. Sumner (1972)

investigate tectonic activity at the head of the Gulf of California. Figure 3 shows a total field, residual aeromagnetic map of this area.

## GEOLOGY

More than 49 years ago, Wegener (1924) proposed that the formation of the Gulf of California was due to the separation of the peninsula of Baja California from mainland Mexico. This proposal was ignored for several decades until development of the plate tectonic theory. Within this concept, it is apparent that the Gulf of California is part of the active boundary between the Pacific and North American plates.

Although the north end of the Gulf of California is 100 km south of the International Border, the structural trough characterized by the Gulf continues northwest to San Geronio Pass, another 300 km. This part of the trough is filled by sediments derived both from the surrounding mountains and from the Colorado River. The trough is bounded on the north by the Transverse ranges, on the west by the Peninsular ranges, on the east by the Colorado and Sonoran Deserts, and on the south by the Gulf of California.

The area of this study is the southern part of the land at the head of the Gulf of California (Fig. 4). Here the trough is filled by combined fan deposits and the delta of the Colorado River. The river has taken different paths across its deltaic cone, at times emptying into the gulf and at times emptying into the Salton Sea (Kovach and others, 1962).

Very little is known of the geology of the delta on the Mexican side. The geology of the northern part of the trough was best summarized by Dibblee (1954). Perhaps the most complete map of Baja California is

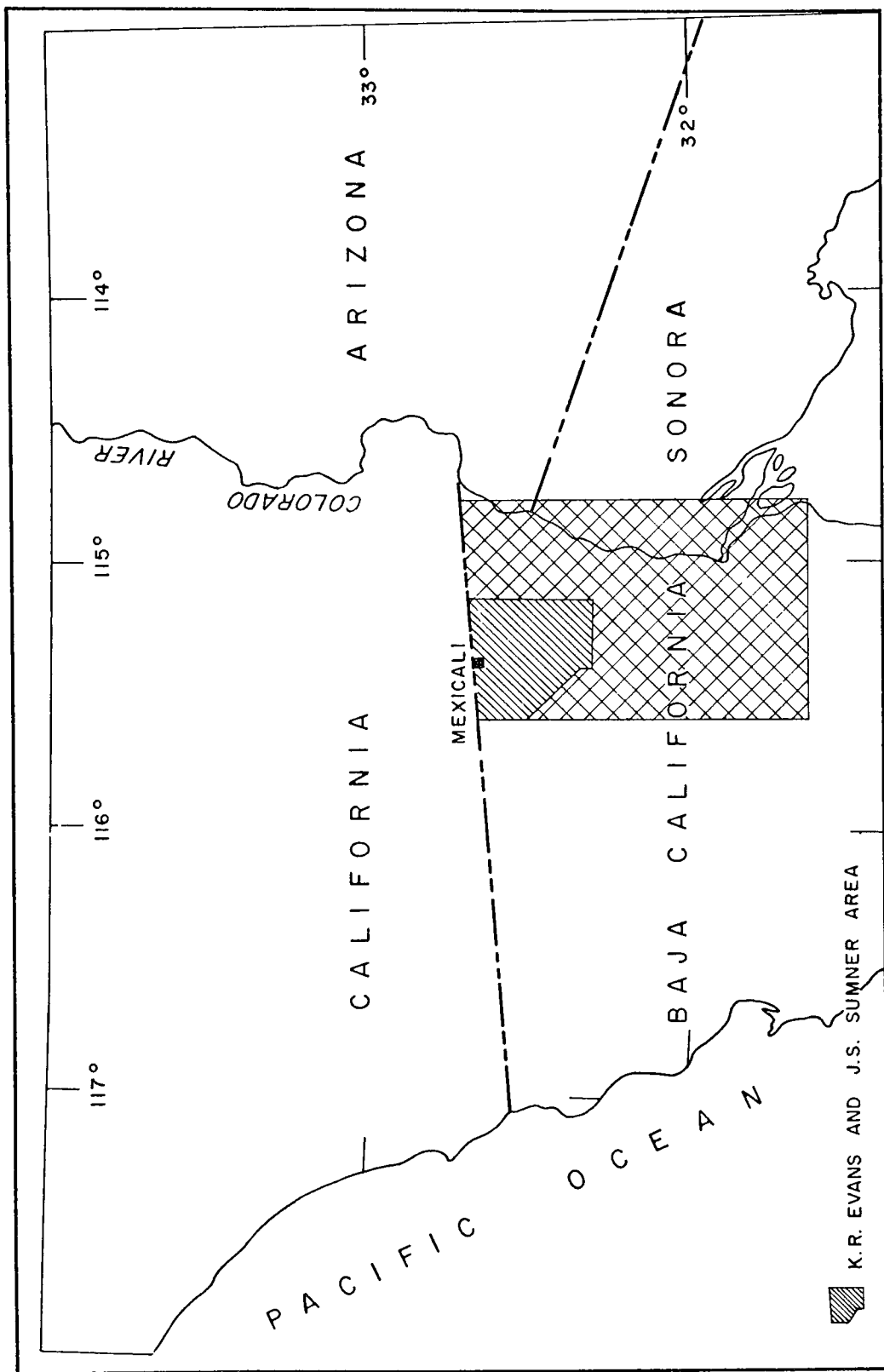


Figure 4. Location of the Colorado River Delta Area, Mexico



the reconnaissance geologic map of the State of Baja California by Gastil, Allison, and Phillips (1971), reproduced as Figure 5.

The stratigraphic column shown on Figure 6 (Kovach and others, 1962) shows the upper Tertiary and Quaternary sediments which fill the trough. The column includes some sediments of marine origin produced by marine incursions. This column could have lateral changes, especially in the west side of the trough where sediments from the Sierra de los Cucapas and Sierra del Mayor interfinger with the sediments of the Colorado River to the east. For example, the deepest well drilled at the Cerro Prieto geothermal field, M-3, encountered granitic basement rock at a depth of 2,532 meters but no overlying marine sediments (Alonso E. and Mooser, 1964).

Crystalline rocks are found in the area in the Sierra de los Cucapas, Sierra del Mayor, and further south in the Sierra de Pintas and Sierra de la Tinaja. The northern part of the Sierra de los Cucapas and the Sierra del Mayor are underlain by plutonic rocks of the great mid-Cretaceous batholith of southern California, whereas the southern part of the Sierra de los Cucapas is composed of Paleozoic(?) pre-batholithic metasediments. Sierra de Pintas and Sierra de la Tinaja are composed of pre-batholithic metasediments and post-batholithic volcanic rocks. The volcanic activity has continued into Quaternary time. This is evidenced by the well-preserved crater of Cerro Prieto and by the obsidian domes at the southern end of the Salton Sea.

The Colorado River delta area lies essentially within the San Andreas fault zone and is highly faulted and structurally complex. The principal structural breaks seen from surface mapping are the

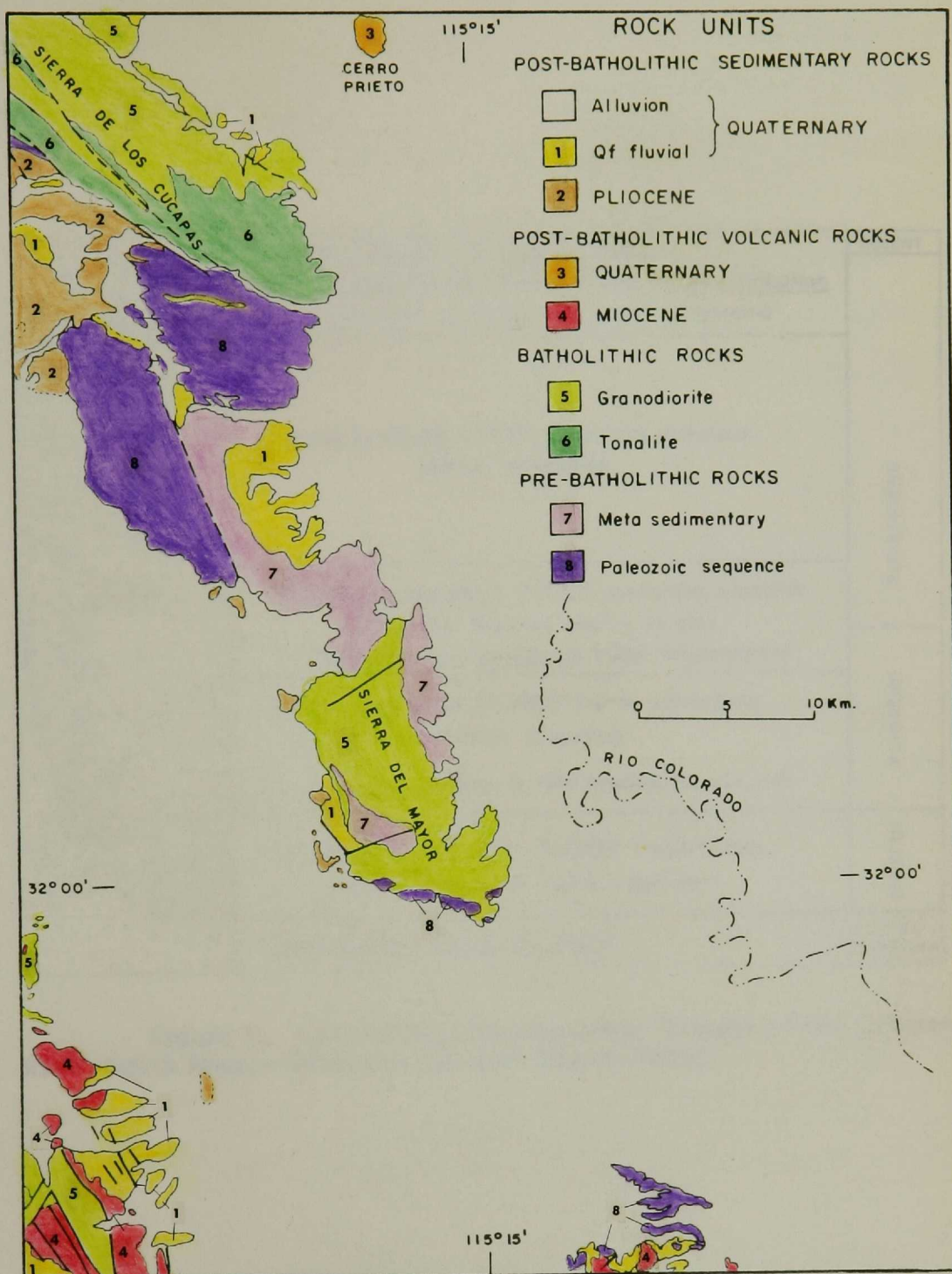


Figure 5. Reconnaissance Geologic Map of the Mexicali Trough.--Modified from Gastil and others (1971)

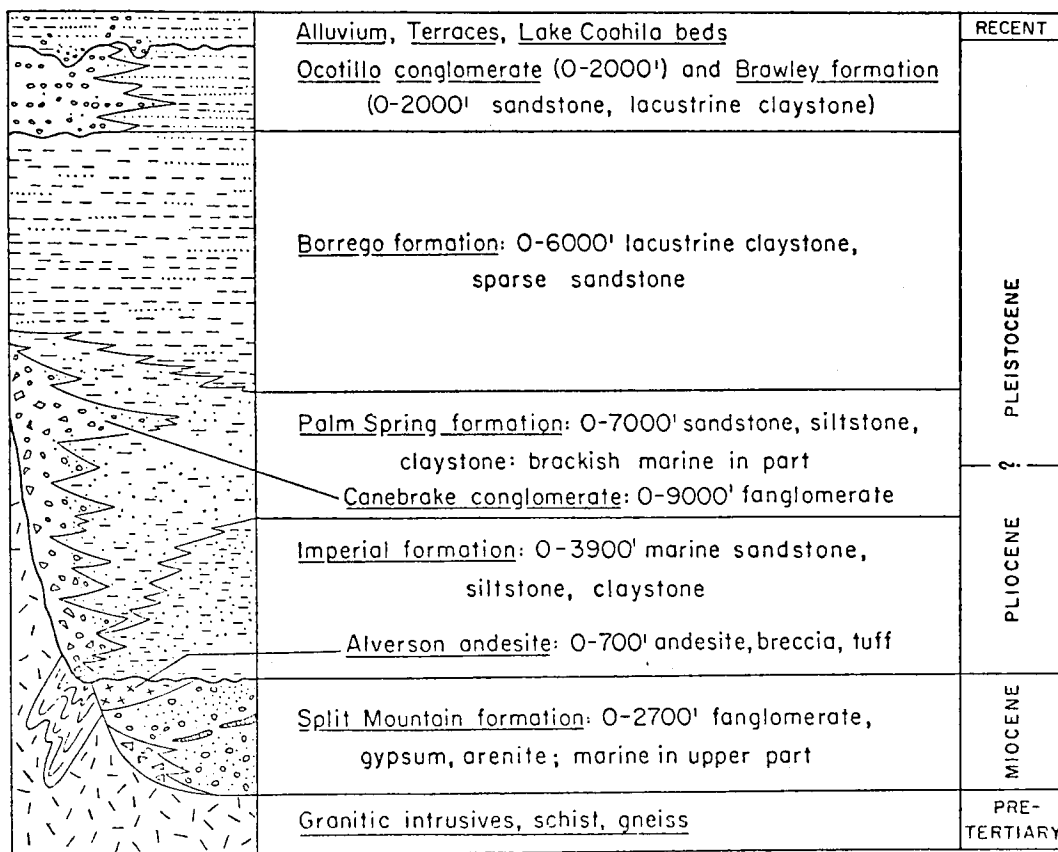


Figure 6. Generalized Stratigraphic Column of the Colorado River Delta Area.--After Kovach and others (1962)

Banning-Mission Creek, San Jacinto, Imperial, Elsinor, and Laguna Salada faults (Fig. 7). Other faults have been inferred by geophysical methods (Elders and others, 1972), and undoubtedly there are many more to be detected. All these faults have a northwesterly trend and are strike-slip faults.

The relationship of the strike-slip faults with spreading centers has been proposed by Lomnitz and others (1970). Figure 8 shows the proposed locations of the spreading centers and the resulting extensional compensation. The location of the rhombochasms proposed by Lomnitz and others has been made on the basis of seismic activity, and the strike-slip faults of the system have sometimes been inferred. Evidence of recent volcanic activity, for example, Cerro Prieto and Obsidian Butte, has also been used to locate the spreading centers in accordance with a model of rifting and magma generation (Elders and others, 1972). Also, the relation between the spreading centers and the geothermal areas in the delta has been used by these workers to propose more complicated patterns of spreading centers.

The magnetic response of the spreading centers in the Gulf of California has been interpreted by J. R. Sumner (1971) as a subdued magnetic anomaly due to the great thickness of sediments which covers the spreading centers. A similar response could be expected in other areas where deltaic sediments cover the spreading centers.

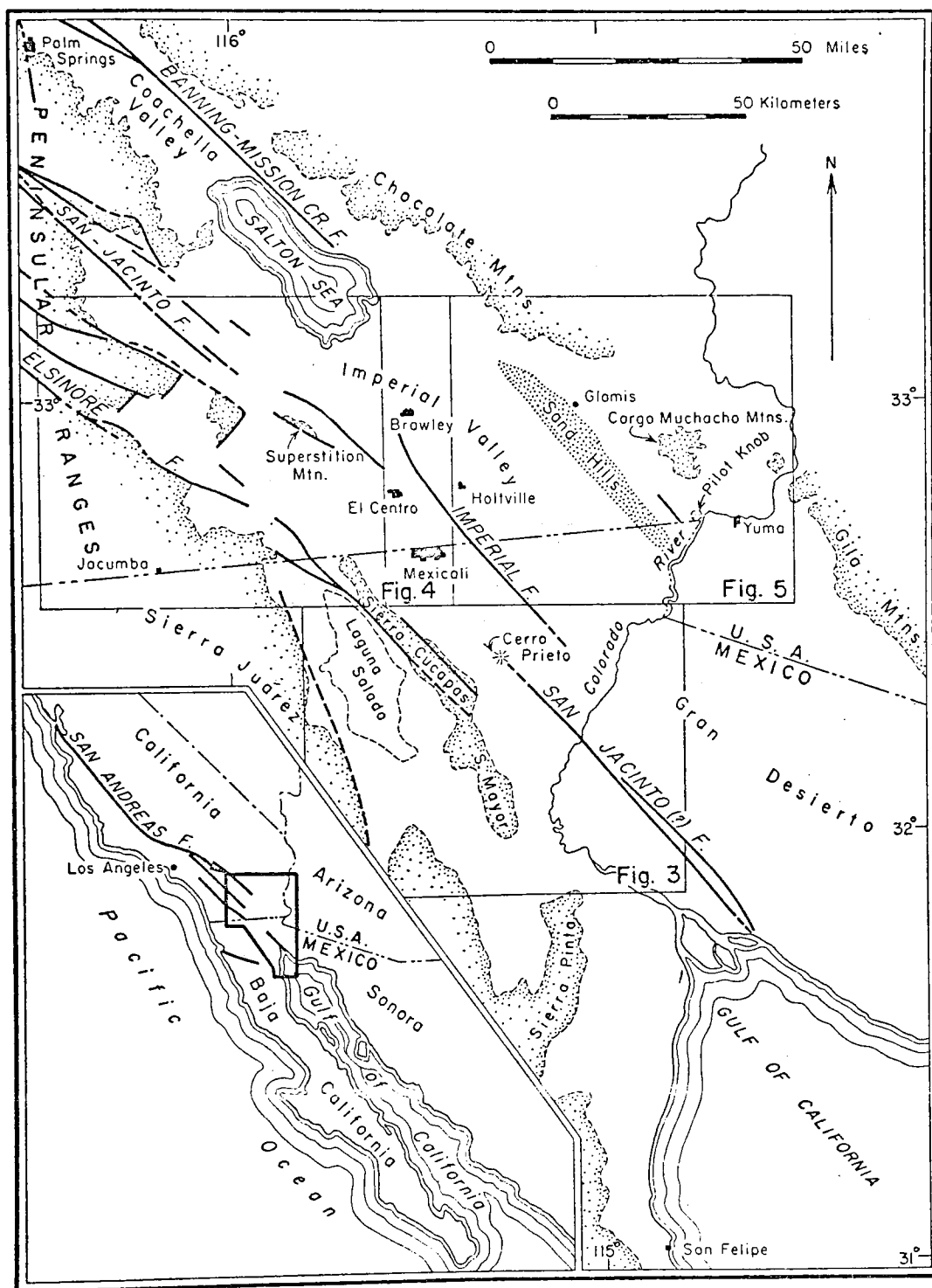


Figure 7. Map of the Colorado River Delta Area Showing Location of the Major Strike-slip Faults.--From Kovach and others (1962)

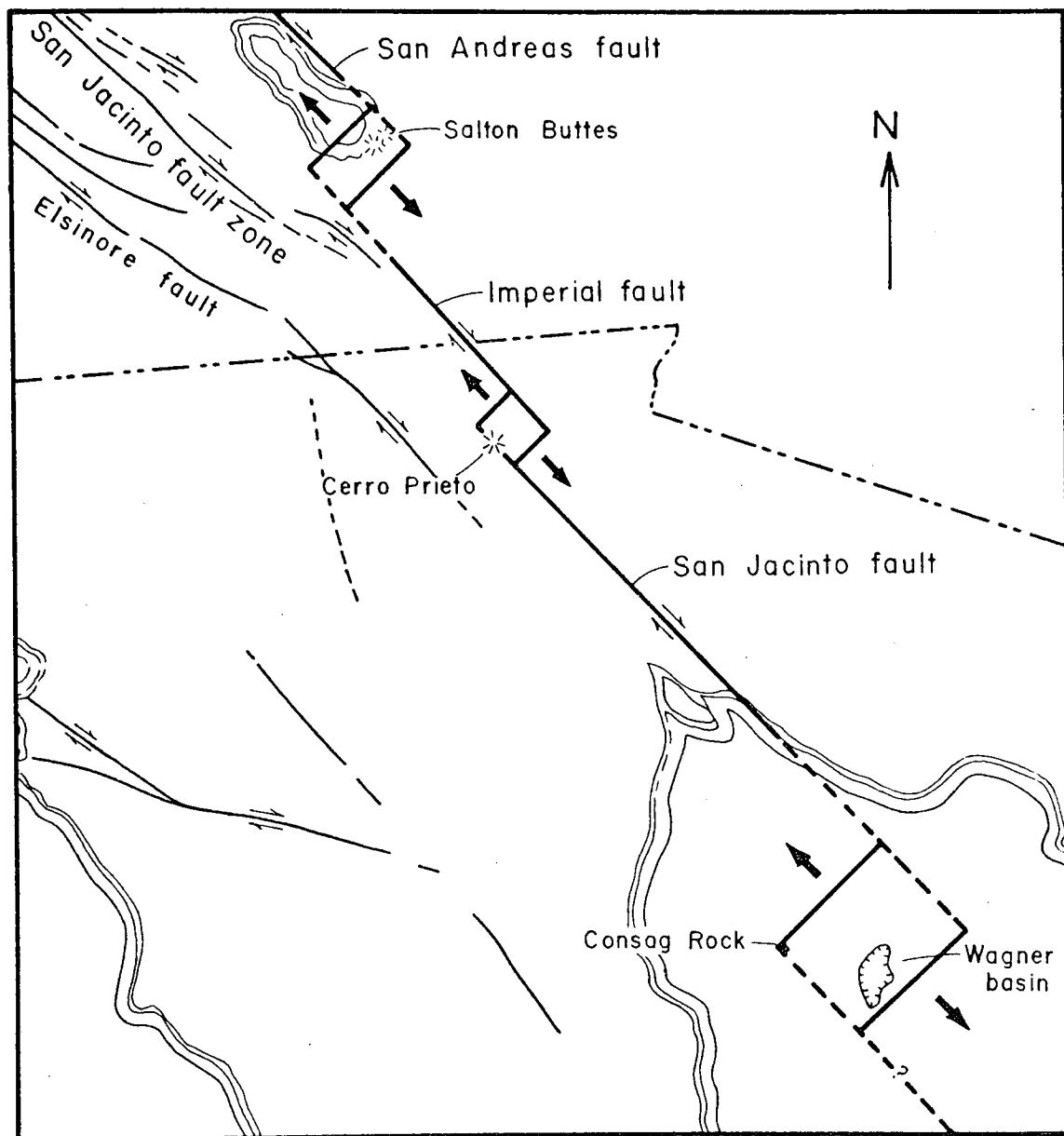


Figure 8. Idealized System of Spreading Centers and Compensating Right-lateral Strike-slip Faults in the Colorado River Delta Area. --After Lomnitz and others (1970)

## THEORETICAL BASIS OF THE AEROMAGNETIC METHOD

### Rock Magnetism

The magnetism of rocks is due partly to induced magnetization which is dependent on the earth's magnetic field and partly to remanent magnetization which is independent of the earth's magnetic field. The induced intensity also depends upon the magnetic susceptibility of the rock. The remanent magnetization is related to the geological history of the rock.

According to the general classification of types of magnetism, rocks are placed in three categories: diamagnetic, paramagnetic, and ferromagnetic. The magnetic susceptibility of a diamagnetic body is negative and the induced magnetization is in a direction opposite to the magnetizing field. Among the many rocks and minerals that show net diamagnetism are quartz, marble, graphite, and rock salt. The susceptibility of a paramagnetic body is positive and decreases inversely proportional to the absolute temperature (Curie-Weiss law). Pegmatites, gneisses, and dolomites are examples of rocks classified as paramagnetic. Ferromagnetic materials, in which the magnetic moment of groups of atoms are aligned in the same direction even in the absence of an external field, have large magnetic susceptibilities; there are no truly ferromagnetic rocks or rock-forming minerals. The temperature at which a material ceases to be ferromagnetic is the Curie temperature for that material, or Curie point.

Magnetite ( $\text{Fe}_3\text{O}_4$ ) is the most important mineral in determining the magnetic characteristics of rocks because it has a high magnetic susceptibility and because it is the most common magnetic mineral. Other important magnetic rock-forming minerals are hematite and ilmenite.

A simplified empirical relationship giving the susceptibility of a rock in terms of magnetite is given by Garland (1971):

$$K = 3000 \times 10^{-6} \text{ (volume percent magnetite).}$$

Table 1 is a compilation of susceptibility as a function of rock type. The table shows that sedimentary rocks can be ruled out as possible sources of significant magnetic anomalies. The susceptibilities of igneous rocks generally increase as the rocks become more mafic. Because the susceptibility of a metamorphic rock depends on the susceptibility of the parent rock and the degree of metamorphism, it is highly variable.

Remanent magnetization of rocks is for the most part a thermoremanent magnetization (TRM) acquired during the cooling process of the rock, and its orientation reflects the orientation of the geomagnetic field at the time of the formation. The predominant mechanism in the acquisition of TRM is the alignment of the domains in the ferromagnetic constituents of the rock. This is particularly true for the igneous rocks which cool in place. In sedimentary rocks, magnetic grains with previous thermoremanence may be deposited with other minerals and mechanically rotated during deposition so that the axis are parallel to the ambient magnetic field. The relationship between induced and remanent magnetizations is known as the Koenigsberger ratio (Q) which is defined as  $J_r/J_i$ , where  $J_r$  is the intensity of remanent magnetization and  $J_i$  is the intensity of induced magnetization.



Table 1. Magnetic Susceptibilities of Some Common Rock Types.--  
Modified from Sauck (1972)

Rock Type	Number of Samples	Range (cgs units x 10 <sup>-6</sup> )	Average
Dolomite	66	1-75	8
Limestone	66	2-280	23
Sandstone	230	1-1665	32
Shale	137	5-1478	52
Rhyolite	44	50-1120	280
Granite	31	28-2700	470
Felsic igneous	58	3-6527	647
Dacite	5	110-1750	830
Gabbro	37	68-5610	990
Andesite	2	950-1700	1320
Diabase	19	64-4200	2590
Mafic igneous	78	44-9711	2596
Basalt	37	480-10000	2950
Metamorphic	61	0-5824	349

High values of  $Q$  are found in extrusive rocks, such as are found in the oceanic crust, in which fast cooling rates dictate growth of only small magnetic grains and result in high remanent magnetization. Low values of  $Q$  are found in intrusive rocks and in sedimentary rocks. The relationship between the grain size of a rock and its remanent magnetization can be explained as a result of the anisotropy of the grain. If the grain is small compared with the thermal agitation, for a given temperature, the grain behaves as superparamagnetic, that is, it exhibits the properties of paramagnetism but with larger individual moments (Garland, 1971).

Since this study is concerned with the interpretation of the crystalline basement structure whose remanent magnetizations can be assumed to have the low Koenigsberger ratio characteristic of plutonic rocks, remanent effects can be ignored.

### Geomagnetic Field

The magnetic field measured at the surface of the earth is a combination of magnetic fields produced by different sources and therefore has both spatial and temporal variations which must be compensated for in compiling a magnetic map.

Spatial changes of the magnetic field are produced by changes in the earth's main magnetic field and by induced magnetic fields. The main magnetic field is the natural field of the earth and can be expressed to a first approximation by an equation for the dipole field or more exactly by an array of spherical harmonic coefficients (Cain and others, 1964). Induced magnetization has the direction of the main magnetic

field, and it is produced in rocks containing magnetic minerals between the surface of the earth and the Curie depth, 16 to 25 km deep, depending on the geothermal gradient. The changes in this magnetization are due to differences in rock susceptibilities and crustal inhomogeneities. When a rock cools below its Curie temperature, it obtains a permanent magnetization (remanent magnetization). This magnetization may be independent of the strength and direction of the present magnetic field but it depends upon the strength and direction of the magnetic field at the time of its formation.

There are at least three important types of temporal variations:

1. Secular variations, characterized by a slow decrease in field strength. These are related to the processes which cause the main magnetic field to reverse and to drift westward.
2. Diurnal variation, a 24-hour variation of the magnetic field caused by the stream of charged particles from the sun. This change depends upon magnetic latitude.
3. Irregular variations, due to a very irregular increment in the flux of charged particles from the sun, resulting from magnetic storms which have a duration of many minutes or hours.

## AEROMAGNETIC SURVEY

### Data Collection

The aeromagnetic survey of the Colorado River delta area was flown July 15 and 16, 1971, using a Cessna 180 aircraft in which a Geometrics portable proton precession magnetometer Model G-806 was installed. The sensing head enclosed in a Fiberglas aerodynamic "bird" was towed on a coaxial cable 30 meters below and behind the airplane. The magnetometer had a one-gamma precision and a sampling rate of two seconds. Attached to the magnetometer was an interfacing unit which contained a digital clock and which provided simultaneous output for analog and digital recording. The analog output was displayed on two Rustrak chart recorders at 1,000 and 100 units full scale. The digital output was punched on BCD paper tape. At a fixed interval of 32 magnetometer readings (approximately one minute), the interfacing unit simultaneously punched the time on the digital output and triggered the location camera. The camera, a 35-mm Beattie-Coleman Varitron Model D0-68 with a data recording chamber, was shock-mounted on the floor in the tail section of the aircraft over a sliding hatch in the bottom of the fuselage. The data recording chamber contained a 24-hour clock, a frame counter, and a removable data tab. A prism between the data recording chamber and the film magazine allowed recording of the information in the data recording chamber on the side of each photograph.

The survey was made with a flight-line spacing of 5 km at a constant barometric elevation of 2,000 feet (0.610 km), except over the

mountains located at the west and south of the area where flight elevations were 3,000 feet (0.915 km) and 2,500 feet (0.762 km).

Navigation was from 1:250,000-scale topographic maps having a 10-km grid overprint. Flight lines were drawn on the north-south grid lines and also midway between these grid lines to give the planned line spacing. Two east-west lines were also flown to provide additional control in bringing all flight lines to the same level and to facilitate contouring.

Evans (1972) found that the magnetic readings at his base station located at Imperial, California, and readings recorded at the Tucson Magnetic and Seismological Observatory were very close, so that it possible on magnetically "quiet" days to use the Tucson Magnetic and Seismological Observatory as a monitoring station for this survey. The distance from the center of the area to the monitoring station is approximately 250 miles (400 km).

#### Data Processing

The most time-consuming part of the data processing was recovering locations of the airplane when magnetic data were recorded. Latitude and longitude was determined for each positioning photograph and the location of each magnetometer reading was obtained by linear interpolation between these points. Flight lines were plotted on conventional aerial photographs and transferred to a topographic map with a scale of 1:100,000. Latitude and longitude were scaled from the topographic map. Exact locations of magnetic contours may have discrepancies estimated to be as large as 0.5 km due to data gaps between

flight lines, interpolation between positioning photographs, and location errors from photographs where terrain is nearly featureless.

The original total intensity magnetic field data were corrected for diurnal variations using values, scaled every 15 minutes, from the Tucson Magnetic and Seismological Observatory records. These values were punched on card and removed from the raw data, using a FORTRAN IV computer program.

After the diurnal corrections had been made, the data were edited in data decks containing up to 16 magnetic readings per card and a card containing latitude, longitude, and time.

The International Geomagnetic Reference Field, shown on Figure 9, was removed using a FORTRAN IV computer program derived from the Goddard Space Flight Center (NASA) report X-611-64-316 by Cain and others (1964). The spherical harmonic coefficients and their derivatives used with the program to obtain the International Geomagnetic Reference Field were taken from Cain and Cain (1968). A bias of 500 gammas was added to the data to produce all positive magnetic values.

The residual total intensity map was made by plotting the flight lines on a Universal Transverse Mercator projection at 1:100,000 scale, with the desired 10-gamma contour crossings marked along the flight path. Plotting was from a computer-generated magnetic tape driving an 11-inch CALCOMP incremental plotter. Contouring was done manually by joining equal value marks, as shown in Figure 10.

A summarized flow chart (Fig. 11) shows the various steps taken in making the final aeromagnetic map. The residual total intensity map of

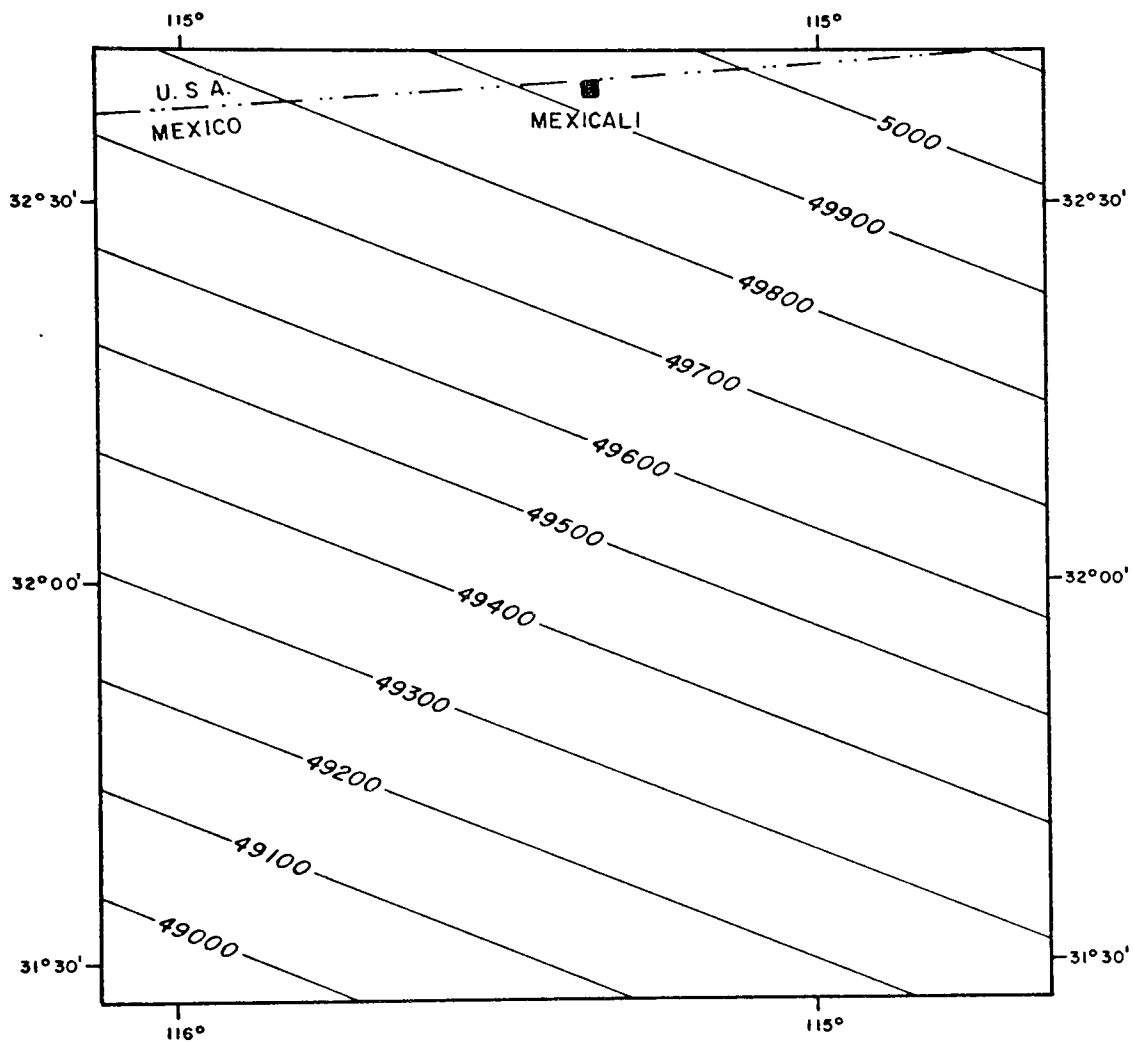


Figure 9. International Geomagnetic Reference Field Which Was Removed from the Original Total Magnetic Intensity Data

Data from Cain and Cain (1968).

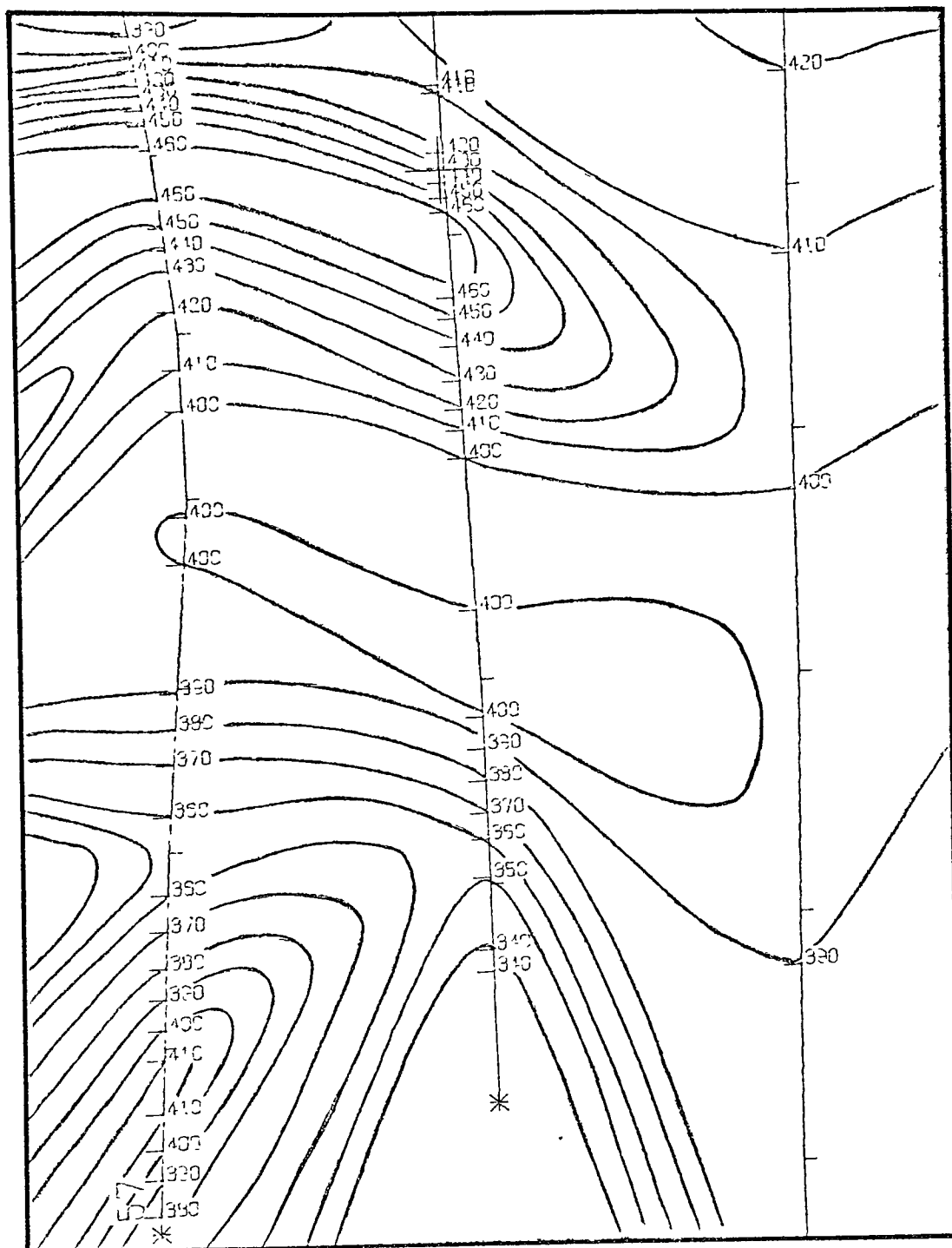


Figure 10. Sample of Computer-generated Plot of Flight Lines with Manual Contouring

Compilation scale is 1:100,000.



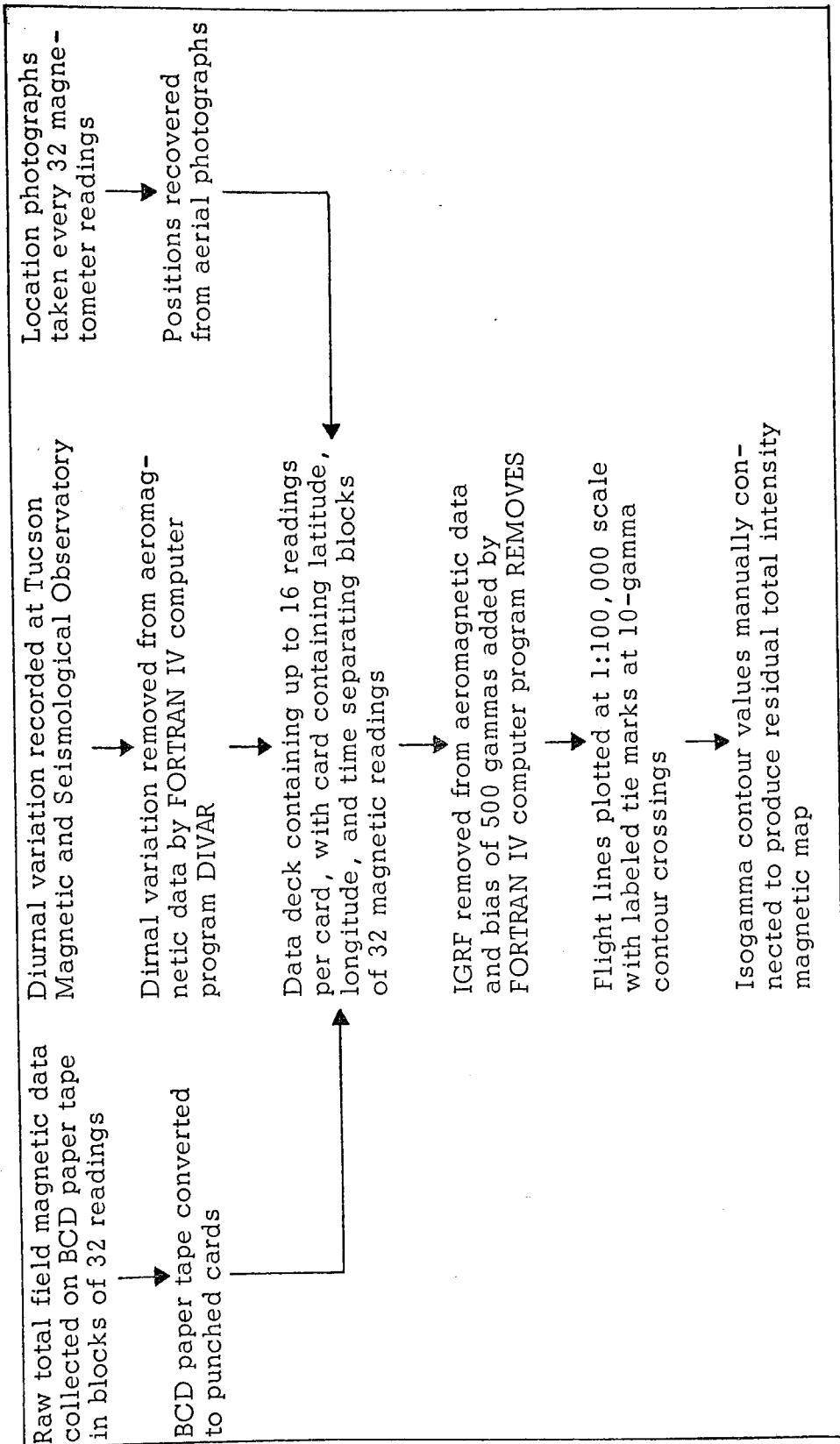


Figure 11. Flow Chart of Procedure Followed in Constructing the Residual Total Intensity Aeromagnetic Map of the Colorado River Delta Area

the Colorado River delta area, reduced to a scale of 1:250,000, is shown in Figure 12 (in pocket).

## INTERPRETATION

An aeromagnetic map without interpretation is of little value. There are different ways of approaching the problem of interpretation; the basic approaches can be classified in two groups: qualitative and quantitative. The qualitative interpretation involves inspection of the map. The quantitative interpretation is used to substantiate the former approach and is based on mathematical processes.

### Brief Description of the Aeromagnetic Map

The aeromagnetic map of the Colorado River delta area (Fig. 12, in pocket) shows a residual magnetic intensity range of 320 gammas, from a high of 540 gammas over the Sierra de los Cucapas (lat  $32^{\circ}15'$  N., long  $115^{\circ}22'$  W.) to a low of 220 gammas over the Sierra de la Tinaja (lat  $31^{\circ}45'$  N., long  $115^{\circ}28'$  W.). A strong northwest trend characterizes the aeromagnetic map.

Broadly speaking, the relatively large amplitude, narrow magnetic anomalies located at the south part of the map have a close relation with the topography and could be interpreted as topographic effects but can also be related to a magnetic contrast in the Miocene post-batholithic rocks (Gastil and others, 1971) from the Sierra de Pintas and Sierra de la Tinaja.

The anomaly located over the Sierra de los Cucapas could also be a topographic effect; this correlation was done using the procedure and graphs developed by Marsh (1971). An important point concerning topographic effects is the absence of magnetic anomalies over the

Sierra del Mayor, where the absence of magnetic anomalies can be related to low susceptibility values. The rest of the area has small-amplitude, long-wavelength anomalies which reflect the basement topography.

The anomaly located at lat  $32^{\circ}2'$  N., long  $115^{\circ}12'$  W. is discussed in the following sections.

### Magnetizations

To obtain a precise interpretation of the aeromagnetic map, it is necessary to know the magnetization of all rock units in the area, but due to the alluvial cover in the delta area, the determination of these magnetizations poses a problem. Stratigraphic control in the delta area south of the International Border is limited to one drill hole in the Cerro Prieto geothermal field (Alonso E. and Mooser, 1964). This lack of stratigraphic control leads to an uncertainty of the basement rock types as well as their susceptibilities. One reasonable assumption is that the basement is composed of rocks similar to those exposed in the Sierra de los Cucapas and in the Sierra del Mayor. As mentioned before, these mountains are formed by metasediments intruded by batholithic rocks.

A few samples were collected in different rock units found in both ranges. The susceptibilities of these samples were measured and none of the samples possessed a significant susceptibility. The low susceptibility of these samples could be related to weathering. A similar observation was discussed by Evans (1972).

Because of this problem, it was decided to use magnetization values for corresponding lithologic units from adjacent areas. Table 2

Table 2. Induced and Remanent Magnetizations for Different Major Rock Units.--After J. R. Sumner (1972)

Rock Unit	Number of Samples	Induced Magnetization <sup>a</sup> (emu/cc x 10 <sup>-6</sup> )	Remanent Magnetization <sup>b</sup> (emu/cc x 10 <sup>-6</sup> )
Granitic and gneissic rocks	17	20-260	175
Miocene(?) extrusive rocks (rhyodacite)	4	0-490	100-150
Pliocene(?) basalts	4	200-650	1000
Metamorphic rocks	7	20-1000	small
Pincate basalt	5	600-1000	2700-4000
Sediments	1	22.3	small

a. In direction of earth's present field (0.5 oersted induced field).

b. Assumed parallel to earth's present field.

shows the range of magnetization values used in the interpretation of the aeromagnetic map.

### Trend Analysis

Under the assumption that the magnetic anomalies over an area reflect to some degree the structural and lithological trends in the crystalline basement, the dominant trends of the magnetic anomalies were studied. However, it is not always possible to determine if a magnetic feature is due to trends in the lithology, to structure, or to a combination of the two.

The method used for the trend analysis was a slight modification of the techniques proposed by Affleck (1963) and Gay (1972). A rose diagram (Fig. 13) was constructed, using primary anomaly trends and gradient lineations. The primary anomaly trends were represented by closed magnetic highs and low. For the geologic trends to be confidently determined from an aeromagnetic survey, they must be at least as long as the flight-line separation (Affleck, 1963), that is, a trend must be at least 5 km long to be compiled. Sixty anomaly trends totaling 1,000 km were plotted on the aeromagnetic map. The azimuth and length of the lines were compiled in 5-degree increments. The length of each 5-degree segment of the rose diagram was determined by adding the lengths of all trends within the azimuth increment, dividing by the total of all trend lengths, and multiplying by 100 so that the trend along a particular azimuth is expressed as a percentage of the total trend.

As can be seen from Figure 13, over 72 percent of the magnetic anomaly trends have a northwest direction. A major trend direction (37.5

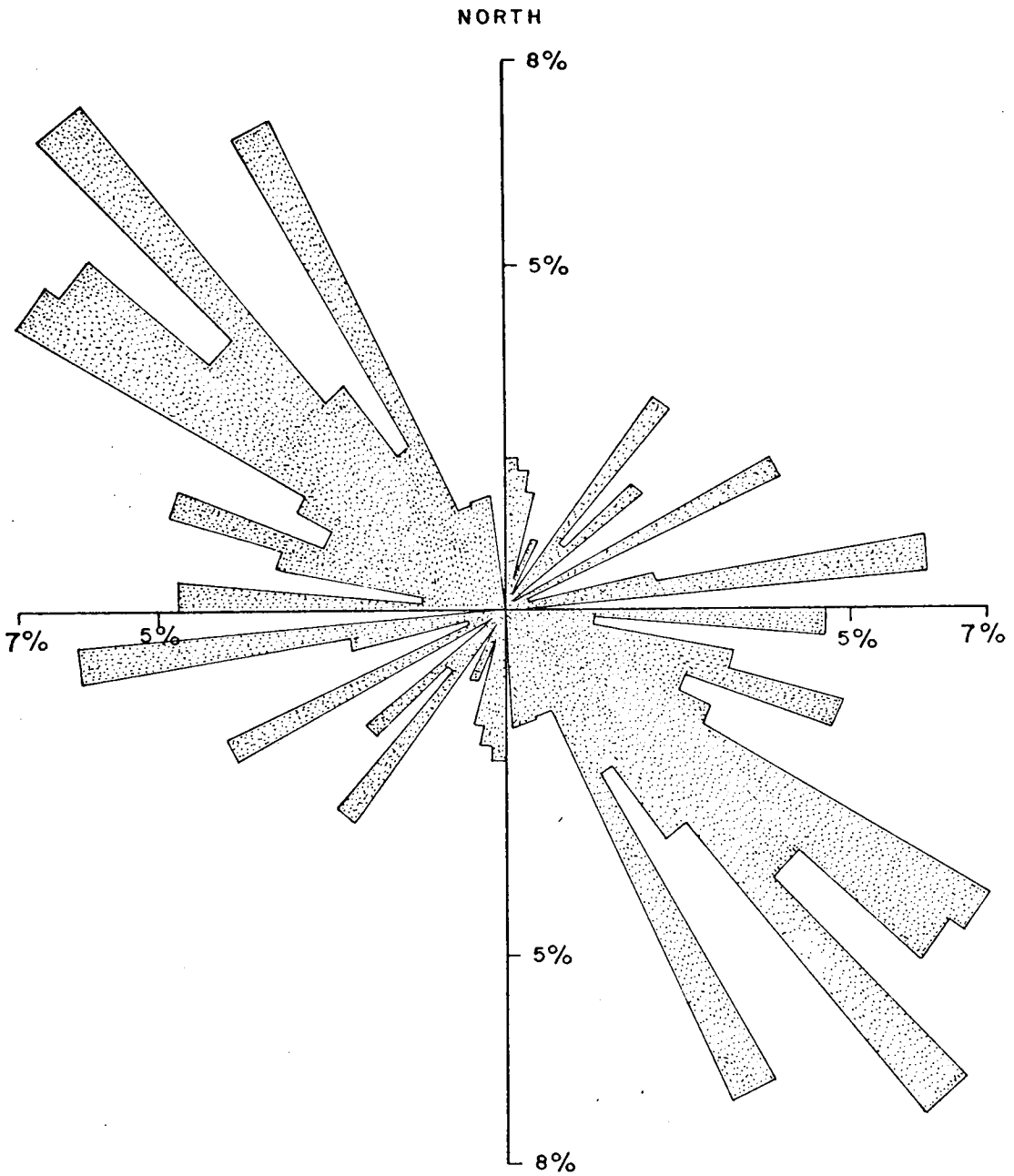


Figure 13. Rose Diagram Illustrating the Results of a Trend Direction Compilation from the Aeromagnetic Map

percent) lies between N.  $30^{\circ}$  W. and N.  $60^{\circ}$  W. and may be interpreted as a reflection of the strike-slip displacements along faults of the San Andreas fault system. The San Jacinto fault, which almost bisects the area, has been geologically mapped with a trend of N.  $40^{\circ}$  W.

Noticeable northeasterly trends are clustered between N.  $75^{\circ}$  E. and N.  $85^{\circ}$  E. (8.5 percent) and between N.  $35^{\circ}$  E. and N.  $50^{\circ}$  E. (7.6 percent). These directions have been interpreted to be a result of the en echelon offset present in the dip-slip and strike-slip faulting.

### Modeling

Perhaps the most important anomaly found with this survey is located at lat  $32^{\circ}2'$  N., long  $115^{\circ}12'$  W. To obtain an idea of its origin a profile A-A' (Fig. 14) was located across the anomaly. Due to the elongate nature of the anomalies in the area, a two-dimensional modeling technique appeared to be the most appropriate, but a problem resulted from the lack of a well-established control for making estimates of depth to basement. The depths used in the modeling of profile A-A' were estimated using Peters' (1949) method. Better depth estimates were desired to minimize uncertainties in the model. A two-dimensional Talwani-type computer program was used for the modeling. This program produces a calculated total intensity profile that can be compared with the observed profile.

For a given magnetic profile over a known basement-sediment interface, any anomalies not due to the basement topography must be due to lateral changes in the susceptibility of the rocks.



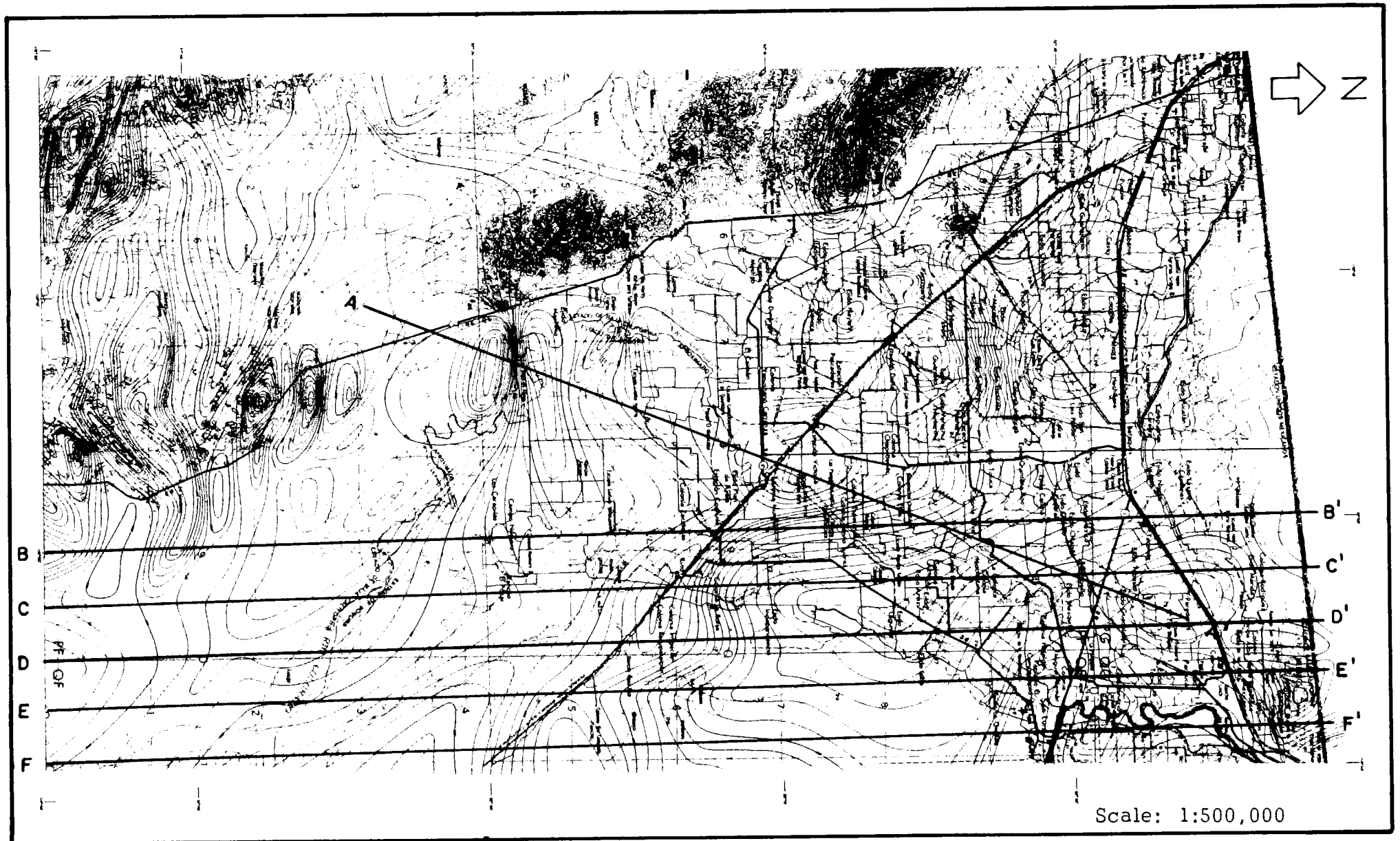


Figure 14. Residual Aeromagnetic Map of the Colorado River Delta Area, Mexico, Showing the Location of the Magnetic Intensity Profiles

A "relief model," a model with no lateral changes in susceptibility, was first attempted. Several models were evaluated using a granitic-type basement of uniform susceptibility, but they did not produce the desired anomaly profile. Thus, it appears that the anomalies in the profile A-A' (Fig. 14) result from a combination of relief and lateral changes in the susceptibility of the basement rocks.

A new model with these characteristics was synthesized. Figure 15 shows the result obtained after many trials for the profile A-A' as well as the observed profile.

The depth to the basement along the profile appears to range between 1,500 and 5,000 meters. The assigned magnetization values, which range from 0.0003 to 0.0006 emu/cc, can be correlated with values of metamorphic rocks, such as those present in the nearby mountains. The magnetization value of 0.0013 emu/cc corresponds to the value of an intrusive pluton. The block with zero magnetization can be interpreted as an effect of alteration produced either by the intrusion or by faulting.

The relatively low magnetization value (0.0004 emu/cc) of the grabenlike structure at the northeast of the intrusive pluton can be interpreted as a result of metamorphic alteration or crustal thinning. This grabenlike structure and the intrusive pluton can be related with the concept of magma generation and rifting normally associated with the formation of a spreading center.

The unit with the value of 0.0006 emu/cc also shows a grabenlike structure, but here there is no change in the magnetization values over the structure, and this structure is interpreted as a product of

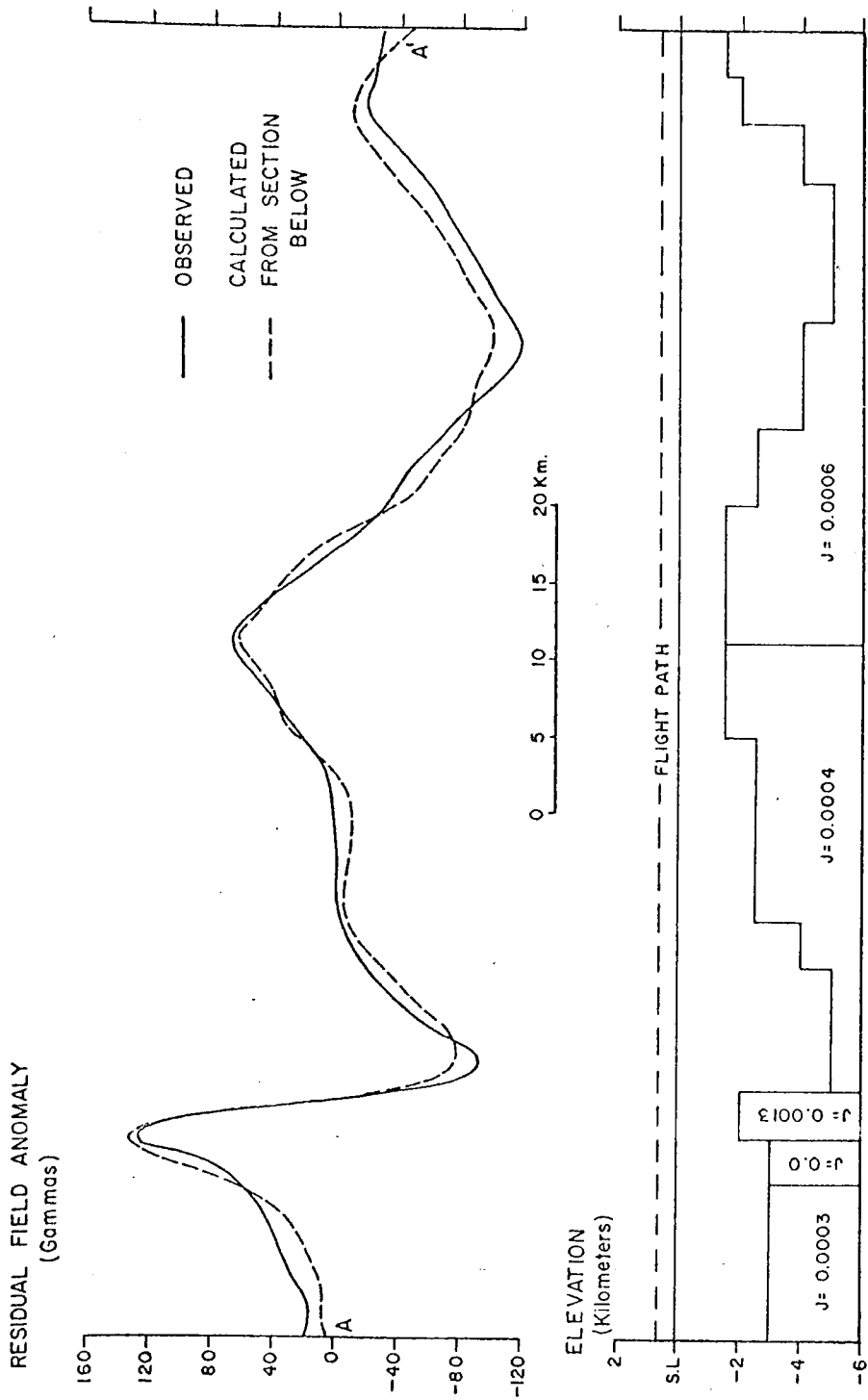


Figure 15. Total Field Profile and Model Geologic Section for Profile A-A'

faulting. The lowest part of this structure corresponds to the deepest part of the Colorado River delta area, as indicated by Kovach and others (1962).

### Crosscorrelation

Crosscorrelation can be defined as the measure of similarity between two functions. If one function is a time or distance shift of the other, the measure of similarity is termed "autocorrelation." The cross-correlation function for two function  $x(t)$  and  $y(t)$  is given by

$$R_{xy}(\tau) = \frac{1}{T} \int_0^T x(t) y(t - \tau) dt$$

(Rex and Roberts, 1969). The computation process is done in the following manner. First, the value of the sample-by-sample product of the two function is computed over the same interval  $T$ ; then the function are displaced relative to each other by a displacement  $\tau$ , and the process is repeated for all values of  $\tau$ . The results are plotted as a function of  $\tau$ . The function  $R_{xy}(\tau)$  has a peak where the functions  $x(t)$  and  $y(t)$  displaced by an interval  $\tau$  match each other in the best possible way.

An alternate method for the calculation of the crosscorrelation function is the use of Fourier transforms. The Fourier transform of the two functions  $x(t)$  and  $y(t)$  is applied to obtain the appropriate spectrums, one spectrum being a complex conjugate multiplied by the other, and the inverse function is calculated. The use of this method may at first seem the long way to calculate the crosscorrelation function, but this method actually requires fewer multiplications than does the calculation of the displaced products directly.

The crosscorrelation method was used under the assumption that it could give the location of a fault if the fault is characterized by a displaced magnetic low. Interpretation is made by plotting the points at which the crosscorrelation function peaks for each combination of functions  $x(t)$  and  $y(t)$  and drawing a line through these points.

It was originally planned to use the values of the total intensity field as obtained from the flight lines, but undesirable variables were introduced into the analysis because these flight line did not keep a constant north-south direction. Instead, five total intensity profiles were scaled from the aeromagnetic map, as shown on Figure 16. The location of these profiles are shown on Figure 14.

A FORTRAN IV computer program, developed by K. L. Zonge (personal communication, 1972), was used to calculate the crosscorrelation functions. This program calculates the crosscorrelation function using the Fourier transform method. It also provides the necessary time and frequency domain filters. Each profile has a total length of 120 km and was digitized in 4,096 sample points. The crosscorrelation between each combination of profiles was calculated. Also, as a proof of the additive characteristic of the crosscorrelation function, profile B-B' (Fig. 14) was crosscorrelated with the rest.

As can be seen on Figure 17, there is a close correlation between the geologically inferred trace of the San Jacinto (?) fault (Fig. 8) and the crosscorrelation points, if the assumption is made that the San Jacinto fault in this part of the area is a fault system consisting of at least two faults. The N. 40° W.-trending San Jacinto fault crosses the profiles B-B' and C-C', but there is no evidence of a fault with this trend

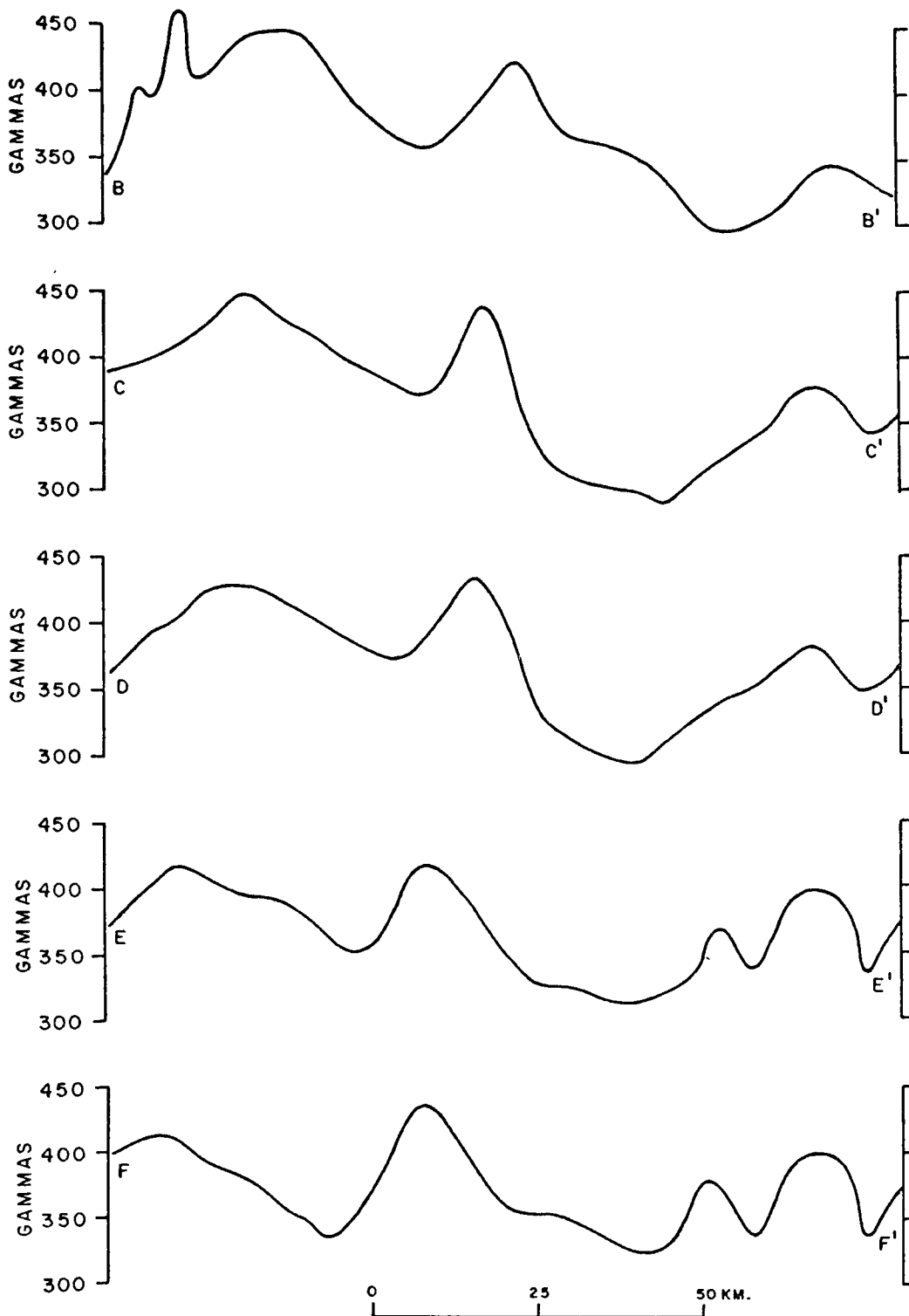


Figure 16. Total Field Magnetic Profiles Used for Cross-correlation Analysis

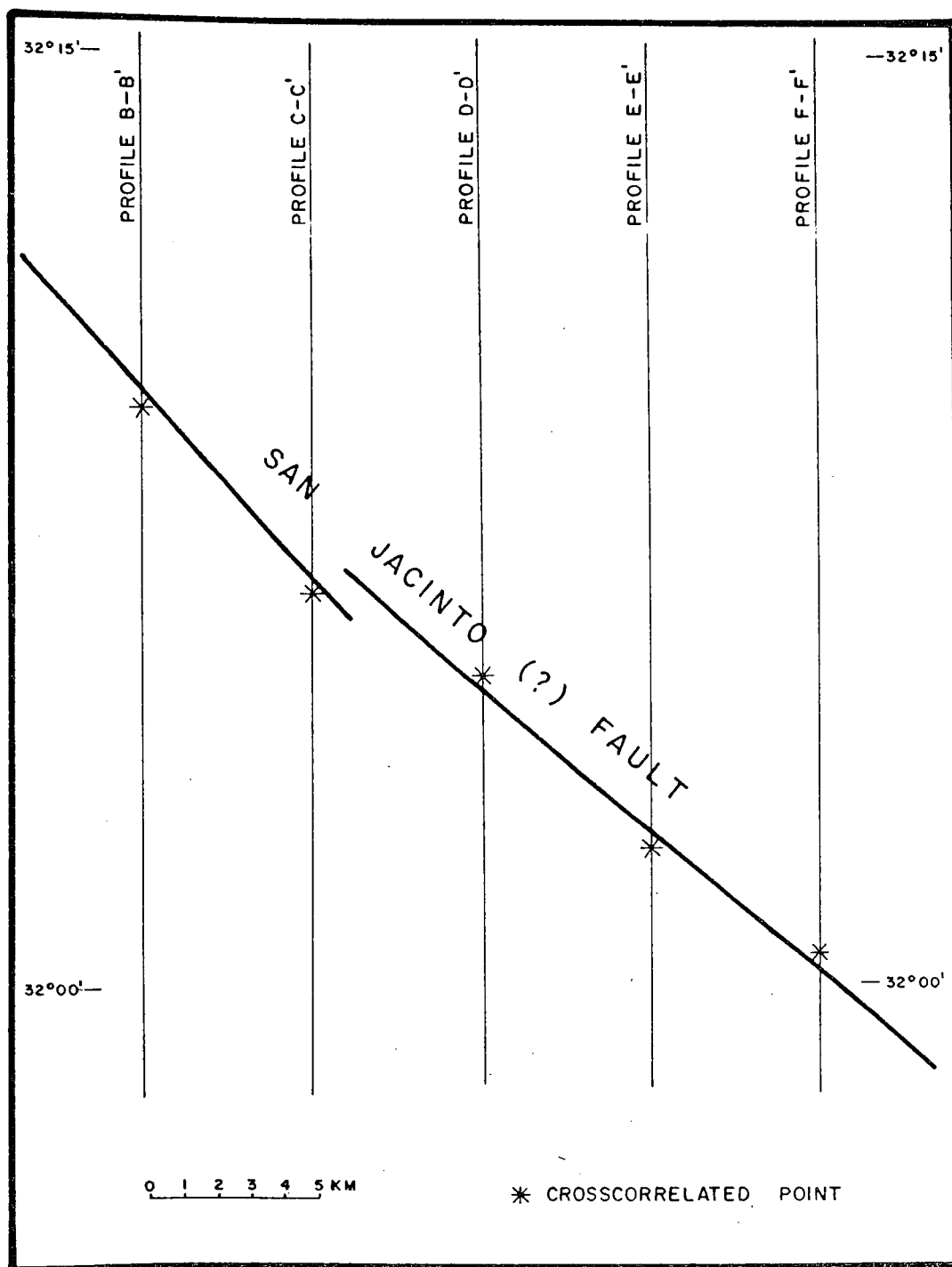


Figure 17. Relation between Geologically Inferred Faults and Crosscorrelated Locations

beyond C-C'. A second fault in the San Jacinto fault system runs almost parallel to the N. 40° W. trend, but it is displaced to the north and does not extend to C-C'.

### Conclusions

The analysis techniques described in this section provide information, which when interpreted according to the theory of global tectonics, leads to the location of a previously unrecognized spreading center in the Colorado River delta area, which is concordant with the system proposed by Lomnitz and others (1970).

In summary, the determination of the location of the spreading center is based on the following evidence:

1. Presence of spreading centers in the immediate area (Lomnitz and others (1970));
2. Presence of an intrusive pluton in the area, such as is commonly associated with a spreading center.
3. Presence of structure in the area which has the same characteristics as those in adjacent areas in which spreading centers have been proposed.
4. Presence of an interpreted grabenlike structure northeast of the intrusive pluton in the model, whose low magnetization could be related to metamorphism, alteration, or to crustal thinning associated with a rifting process.
5. Demonstration by cross correlation that the San Jacinto fault is a fault system of at least two faults in the area.



6. Presence of recent seismic activity (Fig. 18) as reported by Lomnitz and others (1970), which may indicate movement along the faults. More evidence of this seismic activity in the area is provided by Biehler, Kovach, and Allen (1964)

The spreading center interpreted from this analysis is here named Panga de Abajo. The name corresponds to the location of the intrusive pluton. Figure 19 shows the location of the Panga de Abajo spreading center.

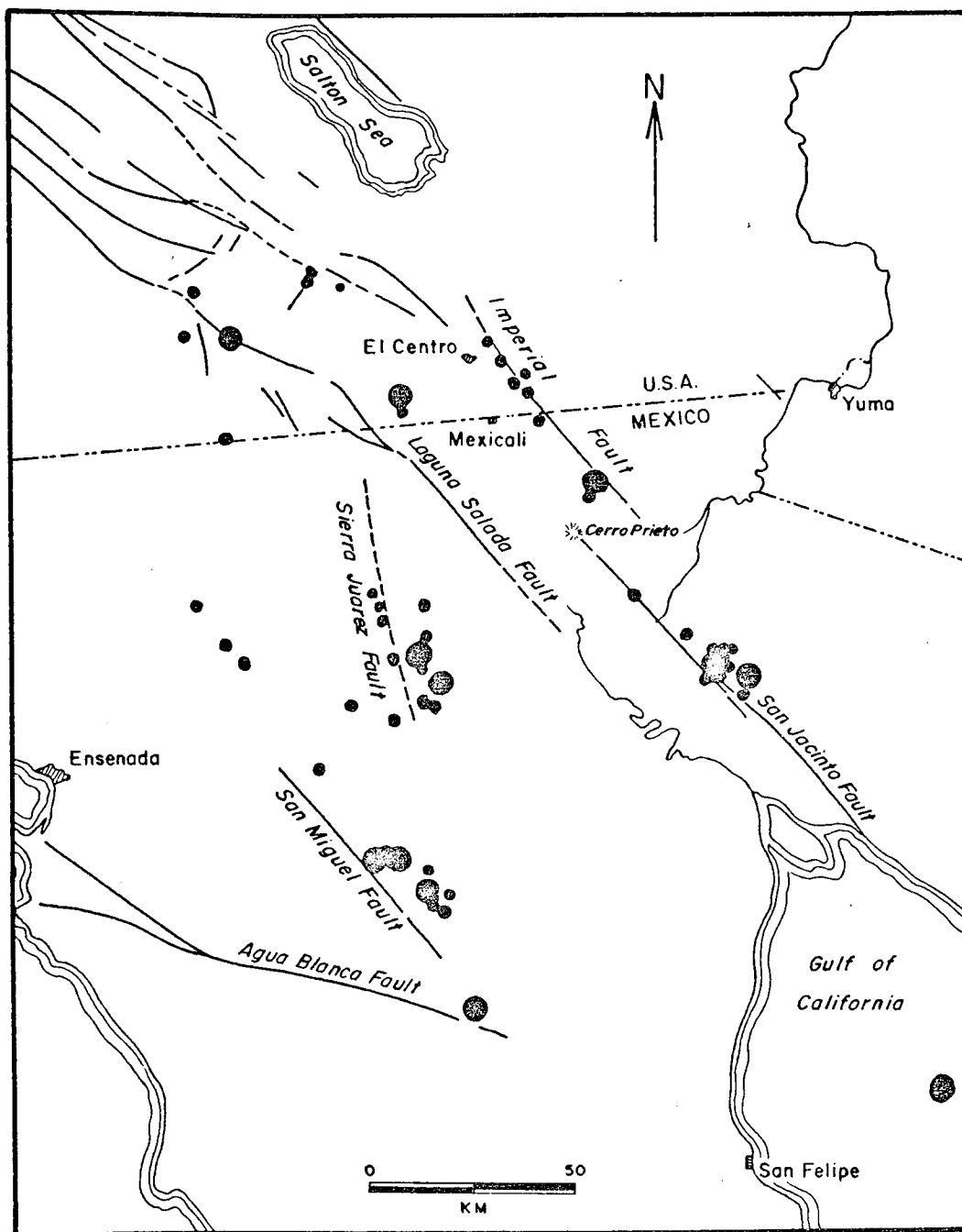


Figure 18. Epicenter Locations in the Northern Baja California Area for Earthquakes Occurring during April and May 1969.--After Lomnitz and others (1970)

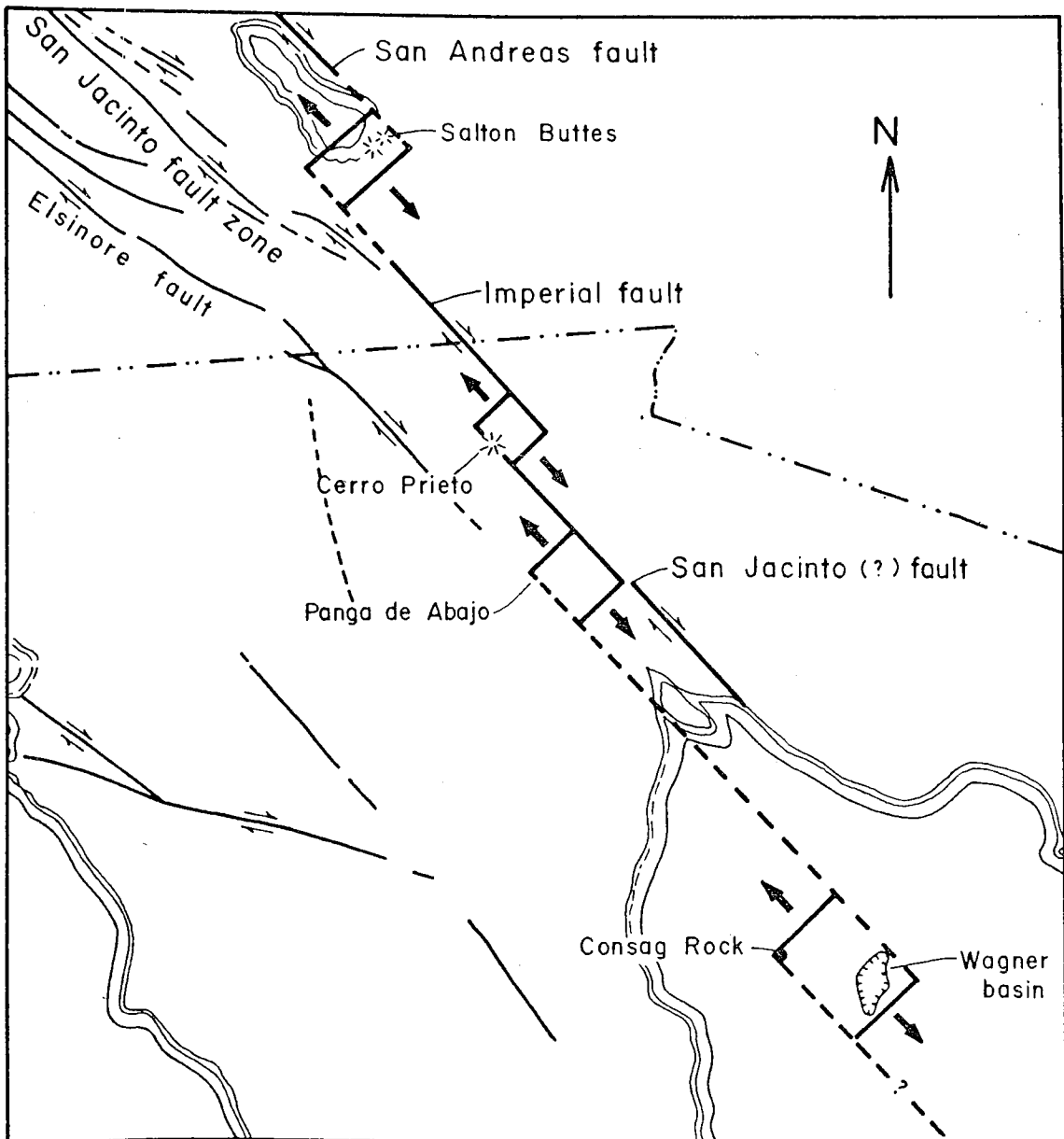


Figure 19. Location of the Panga de Abajo Spreading Center, Baja California, Mexico

The location of the spreading center is related to the idealized system of spreading centers and compensating right-lateral strike-slip faults in the Colorado River delta area.

## RECOMMENDATIONS

Aeromagnetic surveying provides information by which it is possible to estimate the nature of the basement structure beneath great thicknesses of nonmagnetic sediments. Because of the close relationship of basement structure and geothermal sources, aeromagnetic surveying can be considered as an efficient geothermal exploration method. As has been proposed by several authors, it is also an excellent method for studying spreading centers.

The aeromagnetic survey of the Colorado River delta area which is described in this thesis provided enough information to locate a previously unrecognized spreading center which is herein named Panga de Abajo. However, a relationship of this spreading center with a geothermal field, as established for the Cerro Prieto and Salton Sea spreading centers, is not yet proved. The use of more detailed geophysical methods in the Panga de Abajo area is required to determine this relationship.

Within the concept of further geophysical exploration of this area, the gravity and seismic methods must be included. The gravity information available for this area (Kovach and Monges C., 1961) had poor control, and some of the stations could have an error of one mgal or more. There is no seismic information for the immediate area. Data obtained with these two methods can be used to develop a more controlled model of the basement topography.

A magnetotelluric survey of the area can provide valuable information about the depth and extent of a heat source in the area. A

preliminary magnetotelluric survey has been carried out in the Cerro Prieto area in January 1973 (R. Peterson, personal communication, 1973), and the method seems to provide encouraging results.

It is also recommended that a heat-flow study of the area be undertaken, using previous information of the C.F.E. and new measurements. For these measurements, it is possible to use, in some areas, existing water wells, but the necessity of a shallow drilling program at selected places should be considered.

## SELECTED BIBLIOGRAPHY

- Affleck, J., 1963, Magnetic anomaly trend and spacing patterns: *Geophysics*, v. 28, no. 3, p. 379-395.
- Alonso Espinosa, H., and Mooser, F., 1964, El pozo M-3 del campo geotermico del Cerro Prieto, B.C., Mexico: *La Asociacion de Geologos Petroleros Bol.*, v. 16, no. 7-8, p. 163-178.
- Beal, C. H., 1948, Reconnaissance of the geology and oil possibilities of Baja California, Mexico: *Geol. Soc. America Mem.* 31, 138 p.
- Biehler, S., Kovach, R. L., and Allen, C. R., 1964, Geophysical framework of north end of Gulf of California structural province: *Am. Assoc. Petroleum Geologists Mem.* 3, p. 126-143.
- Cain, J. C., and Cain, S. J., 1968, Derivation of the International Geomagnetic Reference Field. A report to IAGA Committee II, Working Group 4: Goddard Space Flight Center prepring X-612-86-501.
- Cain, J. C., Hendricks, S., Daniels, W. E., and Jensen, D. C., 1964, Computation of the main geomagnetic field from spherical harmonic expansions: Goddard Space Flight Center preprint X-611-64-316.
- De Anda, L. F., and Paredes, E., 1964, La falla de San Jacinto y su influencia sobre la actividad geotermica en el Valle de Mexicali, B.C., Mexico: *La Asociacion de Geologos Petroleros*, v. 16, no. 7-8, p. 179-181.
- Dibblee, T. W., 1954, Geology of the Imperial Valley region, California, *in* *Geology of Southern California*: California Dept. Nat. Res., Division of Mines Bull. 170, p. 21-28.
- Elders, W. A., Rex, R. W., Meidav, T., Robinson, P. T., and Biehler, S., 1972, Crustal spreading in southern California: *Science*, v. 178, p. 15-24.
- Evans, K. R., 1972, Aeromagnetic study of the Mexicali-Cerro Prieto geothermal area: unpublished M.S. thesis, University of Arizona, 50 p.
- Facca, G., 1966, La energia geotermica: *Revista Mexicana de Electricidad*, no. 315, p. 35-38.

- Fuller, M. D., 1964, Expression of E-W fractures in magnetic surveys in parts of the U.S.A.: *Geophysics*, v. 29, no. 4, p. 602-622.
- Garland, G. D., 1971, Introduction to geophysics--Mantle, core and crust: Philadelphia, W. B. Saunders Company, 420 p.
- Gastil, G. R., Allison, E. C., and Phillips, R. P., 1971, Reconnaissance geologic map of the State of Baja California: prepared by the students and staff of the Universidad Autonoma de Baja California and San Diego State College.
- Gay, S. P., 1972, Fundamental aeromagnetic lineaments, their geologic significance, and their significance to geology: Denver, Colorado, American Stereo Map Co., 94 p.
- Grant, F. S., and West, G. F., 1965, Interpretation theory in applied geophysics: New York, McGraw-Hill Book Company, Inc., 584 p.
- Griscom, A., and Muffler, L. J. P., 1971, Aeromagnetic map of the Salton Sea geothermal area, California: U.S. Geological Survey,
- Hamilton, W., 1971, Recognition on space photographs of structural elements of Baja California: U.S. Geological Survey Prof. Paper 718, 26 p.
- Horton, C. W., Hemphins, W. B., and Hoffman, A. A. J., 1964, A statistical analysis of some aeromagnetic maps from the northwestern Canadian shield: *Geophysics*, v. 29, no. 4, p. 582-601.
- Koenig, J. B., 1967, The Salton-Mexicali geothermal province: California Div. Mines Geology, Mineral Inf. Ser., v. 20, no. 7, p. 75-81.
- Kovach, R. L., Allen, C. R., and Press, F., 1962, Geophysical investigations in the Colorado delta region: *Jour. Geophys. Res.*, v. 67, p. 2845-2871.
- Kovach, R. L., and Monges C., J., 1961, Medidas de gravedad en la parte norte de Baja California, Mexico: Universidad Nacional Autonoma de Mexico, Instituto de Geofisica Anales, v. 7, p. 9-14.
- Larson, R. L., Menard, H. W., and Smith, S. M., 1968, Gulf of California: A result of ocean floor spreading and transform faulting: *Science*, v. 161, p. 781-784.
- Lomnitz, C., Mooser, F., Allen, C. R., Brune, J. N., and Thatcher, W., 1970, Seismicity and tectonics of the northern Gulf of California region, Mexico. Preliminary results: *Geofisica Internacional*, v. 10, no. 2, p. 37-48.

- Marsh, B. D., 1971, Aeromagnetic terrain effects: unpublished M.S. thesis, University of Arizona, 69 p.
- Moore, D. G., and Buffington, E. C., 1968, Transform faulting and the growth of the Gulf of California since the late Pliocene: *Science*, v. 161, p. 1238-1241.
- Parasnis, D. S., 1972, Principles of applied geophysics: London, Chapman and Hall Ltd., 214 p.
- Peters, L. J., 1949, The direct approach to magnetic interpretation and its practical application: *Geophysics*, v. 14, no. 3, p. 290-320.
- Reford, M. S., and Sumner, J. S., 1964, Aeromagnetism: *Geophysics*, v. 29, no. 4, p. 482-516.
- Rex, R. L., and Roberts, G. T., 1969, Correlation, signal averaging and probability analysis: *Hewlett-Packard Jour.*, v. 21, no. 3, p. 2-8.
- Roth, P. R., 1970, Digital Fourier analysis: *Hewlett-Packard Jour.*, v. 21, no. 10, p. 209.
- Rusnak, G. A., and Fisher, R. L., 1964, Structural history and evolution of Gulf of California: *Am. Assoc. Petroleum Geologists Mem.* 3, p. 144-156.
- Sauck, W. A., 1972, Compilation and preliminary interpretation of the Arizona aeromagnetic map: unpublished Ph.D. dissertation, University of Arizona, 147 p.
- Sumner, J. R., 1971, Tectonic significance of geophysical investigations in southwestern Arizona and northwestern Sonora, Mexico, at the head of the Gulf of California: unpublished ph.D. dissertation, Stanford University, 90 p.
- Sumner, J. R., 1972, Tectonic significance of gravity and aeromagnetic investigations at the head of the Gulf of California: *Geol. Soc. America Bull.*, v. 83, p. 3103-3120.
- Velasco Hernandez, J., and Martinez Bermudez, J. J., 1970, Levantamiento gravimetrico zona geotermica de Mexicali, Baja California: *Consejo de Recursos Naturals No Renovables Bull.* 74, 20 p.
- Wegener, A., 1924, The origin of continents and oceans: New York, Dutton, 212 p.



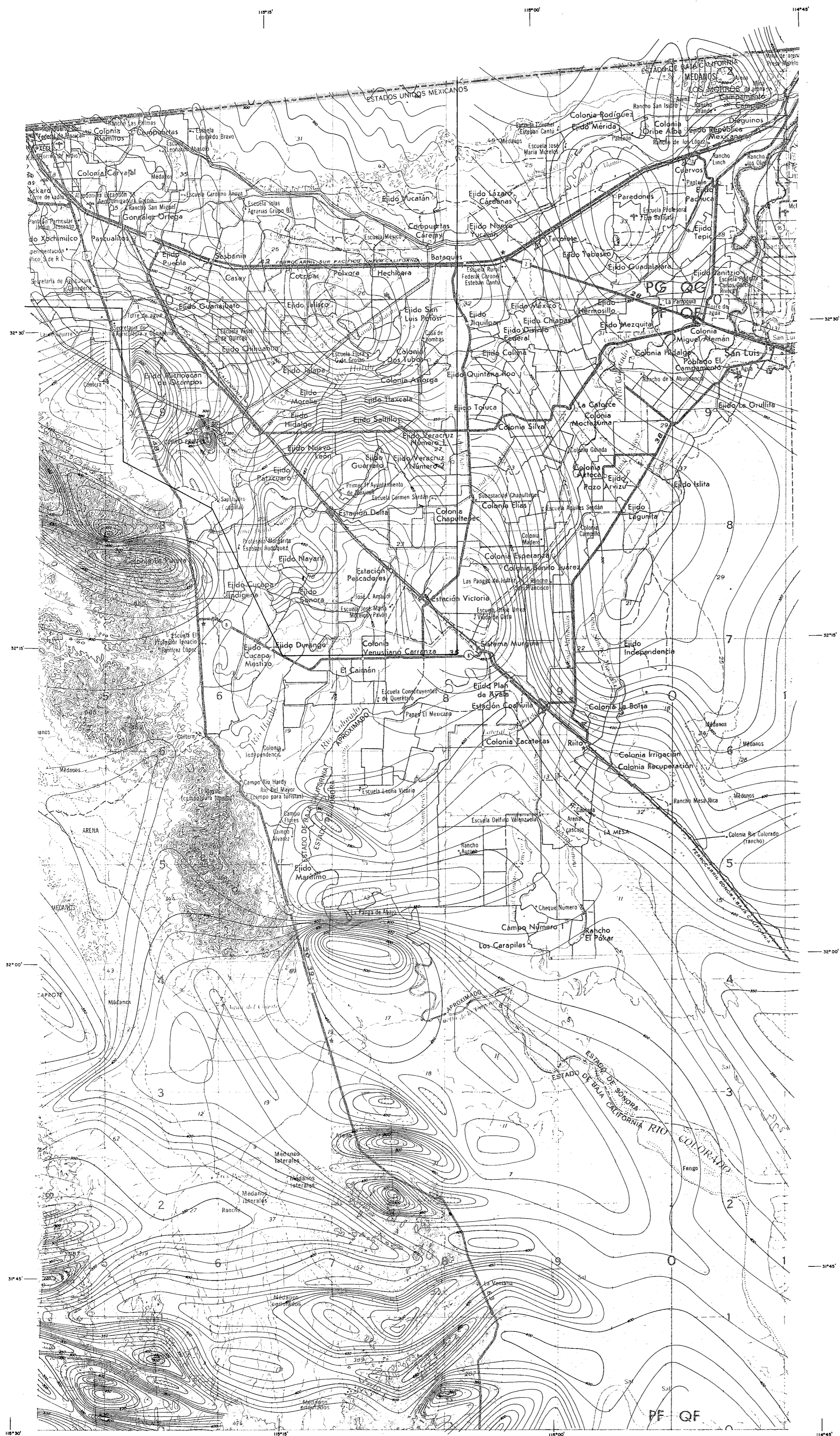


FIGURE 12

**RESIDUAL AEROMAGNETIC MAP  
OF THE COLORADO RIVER  
DELTA AREA, MEXICO.**

**UNIVERSAL TRANSVERSE MERCATOR PROJECTION  
CENTRAL MERIDIAN 115° W, INTERNATIONAL SPHEROID**

**CONTOUR INTERVAL 10 GAMMAS  
BY  
MAURICIO F. DE LA FUENTE AND JOHN S. SUMNER  
LABORATORY OF GEOPHYSICS, UNIVERSITY OF ARIZONA  
1973**

**EXPLANATION**

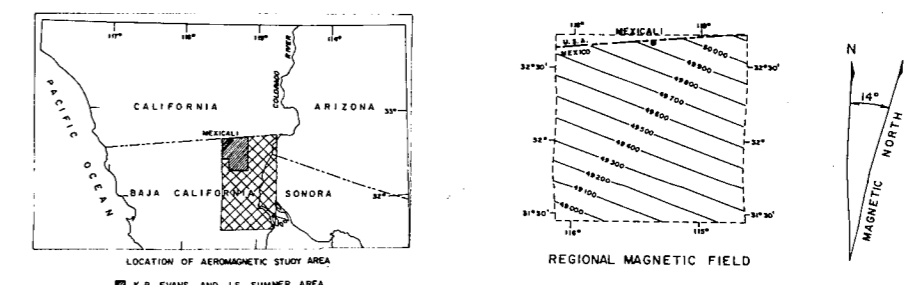
The original total field data were corrected for diurnal variations as observed at the Tucson Magnetic Observatory (EMSA) during the flight period. The regional magnetic field, as shown in the accompanying index map, was removed using a Fortran computer program derived from a Goddard Space Flight Center (NASA) report X-611-64-316 by Cain *et al.*, Oct. 1964. The spherical harmonic coefficients and their first and second time derivatives used with the program to represent the regional magnetic field are from Cain and Cain, 1968. "Derivation of the International Geomagnetic Reference Field. A Report to IAGA, Committee II, Working Group 4" Goddard Space Flight Center preprint X-612-86-501.

The residual values shown on this map are uniformly biased such that the plus 500 gamma contour represents zero residual field.

The Colorado River Delta Area, Mexico aeromagnetic survey was flown July 15 and 16, 1971 with a flight line spacing of 5 km at a constant barometric elevation of 2,000 feet (.61 km) except over the mountains located at the west and south of the area where flight elevations were 3,000 feet (.915 km) and 2,500 feet (.762 km).

The survey instrument was a Geometrics digital recording proton precession magnetometer provided by R. J. Wold of The University of Wisconsin-Milwaukee.

Flight lines were positioned from aerial photographs taken along the flight paths. Exact location of magnetic contours may have discrepancies as large as 0.5 km due to data gap between flight lines and interpolation of locations between positioning photographs. The data used in compiling this map are available.



SCALE 1:250,000

